Design and Fabrication of Customized Hair Clipper Comb

Author

Uzair Ali

Regn Number

00000274205

Supervisor

Dr. Bilal Anjum Ahmed

DEPARTMENT OF MECHANICAL ENGINEERING

COLLEGE OF ELECTRICAL & MECHANICAL ENGINEERING

NATIONAL UNIVERSITY OF SCIENCES AND TECHNOLOGY

ISLAMABAD

August, 2022

Design and Fabrication of Customized Hair Clipper Comb

Author

Uzair Ali

Reg Number

00000274205

A thesis submitted in partial fulfillment of the requirements for the degree of

MS Mechanical Engineering

Thesis Supervisor:

Dr. Bilal Anjum Ahmed

Thesis Supervisor's

Signature: _____

DEPARTMENT OF MECHANICAL ENGINEERING

COLLEGE OF ELECTRICAL & MECHANICAL ENGINEERING

NATIONAL UNIVERSITY OF SCIENCES AND TECHNOLOGY,

ISLAMABAD

August, 2022

Declaration

I certify that this research work titled "*Design and fabrication of customized hair clipper comb"* is my own work. The work has not been presented elsewhere for assessment. The material that has been used from other sources it has been properly acknowledged/referred.

Signature of Student

Uzair Ali

00000274205

Language Correctness Certificate

This thesis has been read by an English expert and is free of typing, syntax, semantic, grammatical and spelling mistakes. Thesis is also according to the format given by the university.

Signature of Student

Uzair Ali

Registration Number

00000274205

Signature of Supervisor

Copyright Statement

- Copyright in the text of this thesis rests with the student author. Copies (by any process) either in full or of extracts, may be made only in accordance with instructions given by the author and lodged in the Library of NUST College of E&ME. Details may be obtained by the Librarian. This page must form part of any such copies made. Further copies (by any process) may not be made without the permission (in writing) of the author.
- The ownership of any intellectual property rights which may be described in this thesis is vested in NUST College of E&ME, subject to any prior agreement to the contrary, and may not be made available for use by third parties without the written permission of the College of E&ME, which will prescribe the terms and conditions of any such agreement.
- Further information on the conditions under which disclosures and exploitation may take place is available from the Library of NUST College of E&ME, Rawalpindi.

Acknowledgments

I am thankful to my Creator Allah Subhana-Watala to have guided me throughout this work at every step and for every new thought which You setup in my mind to improve it. Indeed, I could have done nothing without Your priceless help and guidance. Whosoever helped me throughout the course of my thesis, whether my parents or any other individual was Your will, so indeed none be worthy of praise but You.

I am profusely thankful to my beloved parents who raised me when I was not capable of walking and continued to support me in every walk of my life. I would also like to express special thanks to my supervisor Dr. Bilal Anjum Ahmed for his help throughout my thesis and also for the Advance Engineering Materials course that he has taught me. I would also like to thank Dr. Hassan Aftab Saeed and Dr. Sajid Ullah Butt for being on my thesis guidance and evaluation committee and for their support and cooperation. Without their help, I would not be able to complete my thesis. I appreciate their patience and guidance throughout the whole thesis.

Finally, I would like to express my gratitude to all the individuals who have rendered valuable assistance to my study.

Dedicated to my beloved parents, wife, and siblings whose continuous support and guidance led me to this wonderful accomplishment

Abstract

Prototyping is an essential part of the product design and development process that assists in the implementation of a conceptualized design. 3D-printing has been widely utilized as a prototype method since the 2000s when it became prominent as an additive manufacturing process. The inherent rapid prototyping ability offered by 3D-printing coupled with the need to be able to develop customized daily use applications remains to be the highlight of the present study. This study consists of the development of a hair clipper comb model, impact test analysis, and fabrication of the product using commercially available materials. 3D model of comb for Philips hair clipper was developed using ONSHPAE software, followed by a design study with various materials to understand the impact resistance of the product. The design study was performed via finite element (FE) explicit dynamic mode, where two hair clipper comb designs, one with a solid body and the other with a shell were subjected to drop test simulation in two orientations: leg and head drop. Two readily available 3D-printable plastic materials, Acrylonitrile Butadiene Styrene (ABS) and Polylactic acid (PLA) were selected for the FE simulation while the comb was subjected to free fall from a height of 5 ft (1.67 m). Simulations reveal that the maximum von Mises stress for solid PLA model in head and leg drop configurations are 56.4 MPa and 60.4 MPa respectively, while for the hollow design (shell model), the values are seen to be 40.3 MPa, 30.9 MPa respectively. Similarly, for solid ABS the stress values are found to be 42.8 MPa (head drop configuration) and 34.3 MPa (leg drop configuration) whereas in the hollow model (shell) the values recorded are 30.6 MPa and 26.9 MPa, respectively. To validate the results, the 4 models were fabricated using 3D Printing and were manually dropped from the same height. In line with the simulated results, models prepared from PLA material failed upon the impact while ABS samples having a comparatively better impact resistance sustained the impact without failure. Moreover, fracture surface morphology of the failed PLA component and the surface of ABS in a printed condition were analyzed using Scanning Electron Microscopy (SEM). The microscopic examination was performed to analyze the quality of 3D-printed clipper comb and correlate the

defects with failure mechanism. The shell model made up of ABS material turns out to be the most suitable choice out of the various designs considered.

Keywords: *3D Printing; Drop Test; Scanning Electron Microscopy; Additive Manufacturing; Injection Molding; Finite Element Analysis*

Table of Contents

Declaration iii

Language Correctness Certificate iv

Copyright Statement v

Acknowledgments vi

Abstract 8

List of Figures 12

List of Tables 14

List of Abbreviations and Symbols 15

CHAPTER 1 16

INTRODUCTION 16

1.1 Background, Scope and Motivation: 16

1.2 Research Objective: 19

1.3 Thesis Outline: 19

CHAPTER 2 21

LITERATURE REVIEW 21

2.1 Overview of Additive manufacturing / 3D Printing 21

2.2 3D Printing Techniques: 24

2.2.1 Fused Deposition Modelling: 24

2.2.2 Stereolithography (SLA): 24

2.2.3 Powder bed fusion / Selective Laser Sintering (SLS): 25

2.2.4 Inkjet Printing: 27

2.2.5 Laminated object manufacturing: 28

2.2.6 Direct Energy Deposition: 28

2.3 3D Printing CAD Configuration 31

2.4 Comparison of 3D Printable Material: 32

2.5 Scanning Electron Microscopy: 33
2.5.1 Interaction between Specimen & Electron Beam: 34
2.5.2 Sample preparation for SEM: 35
2.6 Research Gap: 36
CHAPTER 3 37
MATERIALS AND METHODOLOGY 37
3.1 Introduction: 37
3.2 3D Modelling: 37
3.3 Finite Element Analysis: 38
3.3.1 Meshing 38
3.3.2 Material Selection: 41
3.3.3 Analysis Setup: 41
3.4 3D Printing: 42
3.5 Scanning Electron Microscopy: 44
Chapter 4 45
Results and Discussions 45
4.1 Drop test analysis of the PLA model 45
4.2 Drop test analysis of the ABS model: 47
4.3 Drop test of 3D printed PLA & ABS Model 48
4.4 Scanning Electron Microscopy 49
4.5 SEM of fractured PLA 50
4.6 SEM of as printed ABS 51
Chapter 5 53
Conclusion and Future Studies 53
References: 55

List of Figures

Figure 1: Schematic diagram of FDM [6] 17
Figure 2: Evolution of 3D printing industry since 2015 18
Figure 3: Major challenges faced by 3D printing industry in 2019 and 2020 19
Figure 4 : Classification of AM methods based on the type of base materials (FDM, SLS, and SLA) [31] 22
Figure 5: Basic steps in additive manufacturing [35] 23
Figure 6: Schematic diagram of FDM printer [40] 25
Figure 7: Schematic of SLA process [35] 26
Figure 8 : Schematic diagram of SLS process [45] 27
Figure 9: Schematic diagram of inkjet 3D printing [49] 28
Figure 10: Schematic diagram of LOM process [50] 29
Figure 11: Schematic diagram of direct energy deposition [53] 29
Figure 12: Steps of slicing CAD Geometry 32
Figure 13: Schematic diagram of the SEM build structure [59] 35
Figure 14: Schematic diagram of Electron beam and specimen interaction [59] 36
Figure 15: 3D model of hair clipper comb: (a) full model: (b) cut model of solid design: (c) cut model of shell design 37
Figure 16: Meshing: (a) mesh applied on full design: (b) meshing zoomed view 38
Figure 17: Mesh convergence analysis 39
Figure 18: Skewness mesh metrics spectrum 39
Figure 19: Orthogonal quality mesh metrics spectrum 39
Figure 20: Calculated average skewness value 40
Figure 21: Calculated average orthogonal quality value 40
Figure 22: Orientations for drop test analysis: (a) head drop: (b) leg drop 42
Figure 23: Creality Ender-3, 3D Printer 42
Figure 24: 3D printed samples: (a) PLA solid: (b) PLA shell: (c) ABS solid: (d) ABS shell 43
Figure 25: Solid body PLA simulation result: (a) stress distribution while leg drop: (b) stress distribution while head drop 45

Figure 26: Shell body PLA simulation result: (a) stress distribution while head drop: (b) stress distribution while leg drop 46
Figure 27: Solid body ABS simulation result: (a) Stress distribution while head drop: (b) Stress distribution while leg drop.....47
Figure 28: Shell body ABS simulation result: (a) Stress distribution while head drop: (b) Stress distribution while leg drop:.....48
Figure 29: Drop of 3D printed samples: (a) leg drop: (b) head drop: (c) crack originates in solid PLA model 49
Figure 30: SEM images: (a) neat surface of ABS 3D printed part: (b) fracture surface PLA 3D printed part.....49
Figure 31: SEM image acquired from the fractured surface of impact tested PLA sample 51
Figure 32: SEM images acquired from the surface of as-printed ABS sample 52

List of Tables

Table 1: A summary of materials, application, benefits, and limitations of the main methods of additive manufacturing.....30
Table 2 : Commonly used slicing formats for 3D printing 31
Table 3: Summary of materials applications, advantages, and limitations used for 3D printing.....33
Table 4: Mesh details 38
Table 5: Material properties 41
Table 6: 3D printer specifications 43
Table 7. Stress distribution on all design 48

List of Abbreviations and Symbols

Symbols	Abbreviation
AM	Additive manufacturing
IM	Injection Molding
FEA	Finite element analysis
SEM	Scanning electron microscopy
CAD	Computer aided design
PLA	Polylactic acid
ABS	Acrylonitrile butadiene styrene
FDM	Fused deposition modelling
SLA	Stereolithography
SLS	Selective laser sintering
LOM	Laminated object manufacturing
DED	Direct energy deposit
EBM	Electron beam melting
SLM	Selective laser melting
LMD	Laser metal deposition

CHAPTER 1

INTRODUCTION

The research work in this dissertation has been presented in two parts. The first part is related to the detailed study of designing and finite element analysis of component while second part is related to the 3D- Printing and SEM of 3D printed parts. The objective of this study is to design, analyze and the fabrication of component and to characterize surface morphology of 3D printed parts using scanning electron microscopy (SEM).

1.1 Background, Scope, Motivation:

3D printing, also known as additive manufacturing (AM), is an advanced manufacturing method that entails adding materials layer by layer to create 3D objects explicitly from computer-aided design (CAD) models [1]–[5]. In the 1980s, 3D printing was first made available to the general public. Hull [6] designed and patented the first known 3D printer in 1986. In 1989, Crump [7] invented a new type of 3D printing equipment called Fused Deposition Modelling (FDM), which employs a different approach than Hull's printer. Using a photopolymer, Hull illustrate how to make objects by hardening layers of resin. This technique was named Stereolithography which is different from FDM technique presented by Crump [7].

Fused deposition modelling is an additive manufacturing method that develops components layer by layer through heating thermoplastic material to a semi-liquid condition and extruding it via a tiny nozzle in accordance with 3D CAD designs, which are typically in STL format, as illustrated in Fig 1 [8]. The filament is typically circular in cross-section, with particular diameters for each FDM system. The most often seen dimensions are either 1.75 mm or 3.0 mm. Because of the nature of the FDM process, several advantages arise, including the capacity to create complicated forms without the need to invest in dies and molds, as well as the ability to manufacture interior features, which is difficult to do using conventional manufacturing processes. FDM permits the minimization of the number of assemblies by manufacturing unified complicated pieces. The latest developments in technologies of additive manufacturing (AM) for the

production of small to medium components make it a very appealing process to industries with frontier technologies industries [9].

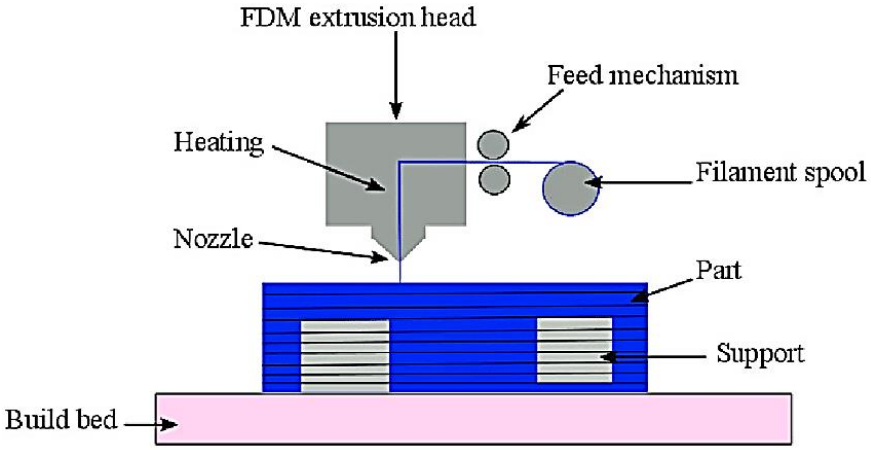

Figure 1: Schematic diagram of FDM [8]

The expanded utilization of 3D printing as a learning tool and to produce practical end-use parts have created the requirement for a better understanding of the mechanical behavior of 3D printed parts and the improvement of scientific apparatuses and plan guidelines for engineers [10]–[12]. Because of the flexibility in geometrical freedom, specifically designed products or components with greater performance may be manufactured, all using 3D printing technology [13].

AM and IM both technologies have few similarities. Both of these technologies are intended to make the designer's vision into reality as effortlessly as could be possible [14]–[16]. Injection molding (IM) is one such conventional manufacturing method that produces parts with molten materials and molds. In mass production, IM is typically employed where parts are to be created thousands or even millions of times. The geometrical complexities of components and the size of the production run limit the use of conventional manufacturing methods consecutively forcing one to use tools or process that rapidly increase the overall cost of produced part [17].

At present, AM technologies competitiveness is well established for small to medium size production volume predominately for plastic components [18]. Parts are not simply transitioned as to maintain the design for conventional process rather redesigned for AM which exploits its capabilities and effectiveness. The adaptability of AM allows it to

accommodate for customized design and geometrical complexities of part providing major competitive advantage over any conventional technique.

This subsequent aspect can also be realized as per the application field: fewer assembly errors, efficient short production runs, ergonomic products, multi-material products, lighter weight products and, therefore, a more sustainable manufacturing process, an optimized use of materials, a combination of different manufacturing process, lower tool investment costs, lower associated cost [19].

In the next few years, AM is deemed to be amongst the key revolutionary industrial process. The use of AM in mass manufacturing is still stalled due to its speed, cost and material choice but due to obvious effect of research and development and progression in technologies, an increase in rapid additive solutions keep emerging. Over the years, these incremental transformations will continue piling up but still, a long road awaits 3D printers to meet the speed of conventional manufacturing processes. AM advantage in flexibility will tip the decision balance in its favor as compared to IM, in case of cost being the same. The evolution of additive manufacturing (AM) in the span of last six years, as documented by Sculpteo [20], have categorized the usage of 3D printing into five major categories: proof of concept, prototype development, production, education, and marketing samples [20]. While protype development remains to be the dominant purpose for which 3D printing has been used in the last six years, utilization of AM for production needs have also seen a continuous upward growth [20] (Figure 2).

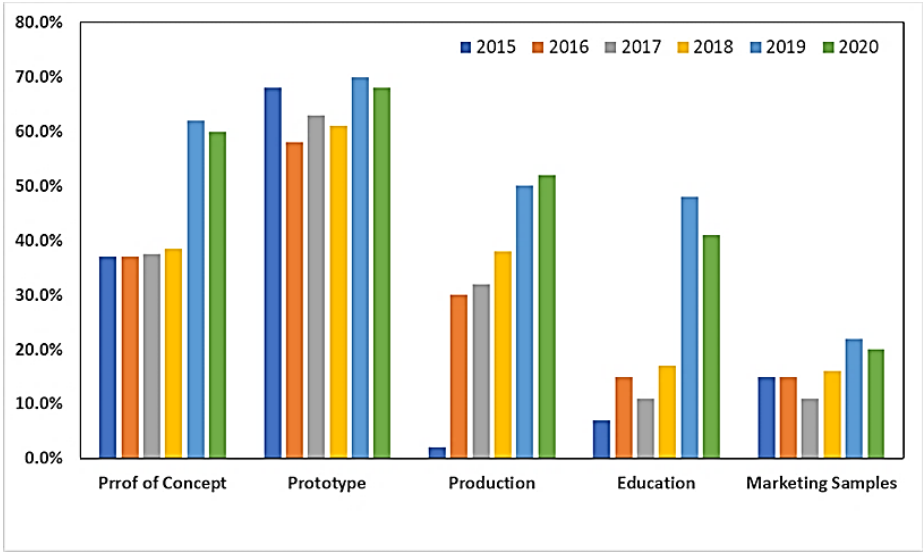

Figure 2: Evolution of 3D printing industry since 2015 [20]

Nevertheless, there is still much work to be done in order for the production industry to fully benefit from AM technology. As per the annual reports published on "State of 3D printing" by Sculpteo in the year 2019 as well as 2020, consistency and quality control remain to be the single most cited challenge faced by the users of 3D printers (Figure 3) [20].

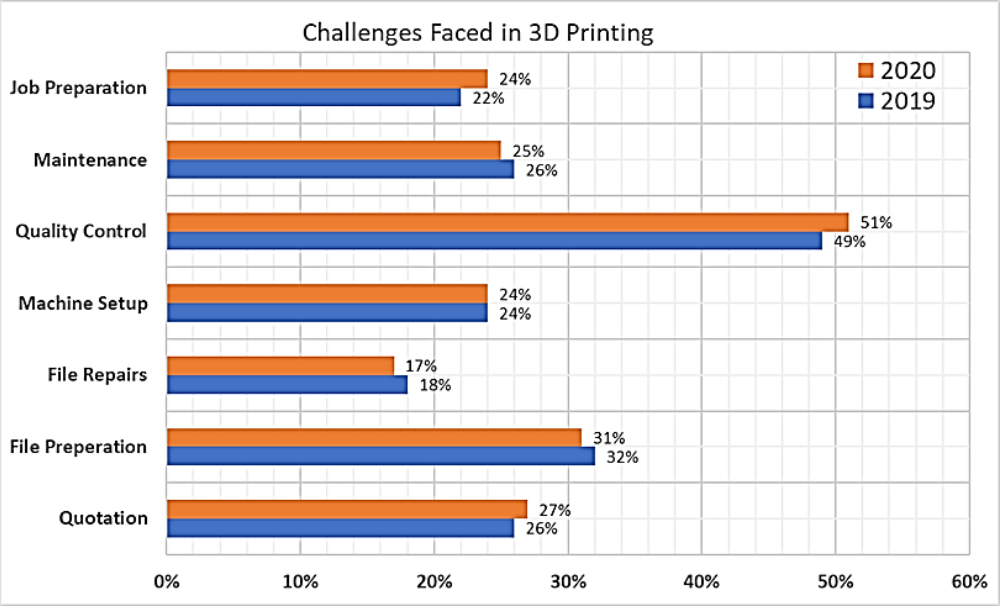

Figure 3: Major challenges faced by 3D printing industry in 2019 and 2020 [20]

1.2 Research Objective:

The objective of the present study is to design a hair clipper comb and assess its suitability to bear impact loading by performing numerical simulations. It is further aimed to identify a suitable thermoplastic polymer for the design and manufacturing of the said component. Lastly, the designed components are to be manufactured using FDM technique and numerical results are to be verified.

1.3 Thesis Outline:

This thesis is divided into five chapters. Chapter 1 presents the introduction, including additive manufacturing technology. A brief introduction to FDM technique which was used in present study is discussed. Chapter 2 discusses the literature review about the types of additive manufacturing technologies. This chapter also discussed the current challenges of 3D printing. Chapter 3 presents the materials and methods, in which the

design of component, numerical analysis on ANSYS (Version 19.2) and the manufacturing of component is discussed. Chapter 4 presents the results obtained from the numerical analysis and the characterization of 3D-printed component. Chapter 5 presents the conclusions drawn from the results, limitations of the current studies and discussion for the future studies.

CHAPTER 2

LITERATURE REVIEW

2.1 Overview of Additive Manufacturing / 3D-Printing

3D printing, also known as rapid prototyping (RP), is an AM technology that is constantly seeking attention in terms of creating lightweight, compact and complicated geometries that seem to be difficult to produce with standard subtractive manufacturing processes like milling, drilling, turning, etc. A variety of factors have contributed to 3D printing's rise in popularity in recent years, including its capacity to make minimal-cost and multipurpose products with sensitive and complicated structures in a short time frame, as well as its unmatched creative flexibility [21]. For example, during 3D printing of concrete materials, the process evolves in the reduction of construction waste by 30-60%, 50-80% less labor costs, and 50-70% less construction time. Therefore, 3D printing is found to be a viable production method in rapid prototyping and engineering sectors including mechanical, civil, aerospace, electronics, and biomedical [22]. A wide range of materials could be 3D printed, such polymers, metals, ceramics, polymer-composites and cement, using a variety of AM techniques [23]–[26].

There are six major kinds of AM processes defined by the ASTM (ISO/ASTM 52900:2015). On the basis of the operation concept, this division covers jetting, binder jetting, photopolymerization in a vat, powder-bed fusion, extrusion, and sheet-lamination. Additionally, AM may be divided into three types according to the kind of base material used: solid, powder, and liquid (Figure 4).

Fused deposition modelling (FDM), laminated object manufacturing (LOM), electron beam free form fabrication and wire & arc additive manufacturing are all examples of solid-based AM. Selective laser melting (SLM), laser metal deposition (LMD), electron beam melting (EBM) and selective laser sintering (SLS) are all powder-based additive manufacturing processes [27]–[31]. The expiration of prior patents has allowed manufacturers to design new 3D printing machines, making this technology more widely

available. Three-dimensional printers are now more affordable, allowing for new uses in educational institutions, and research facilities. Due to its speedy

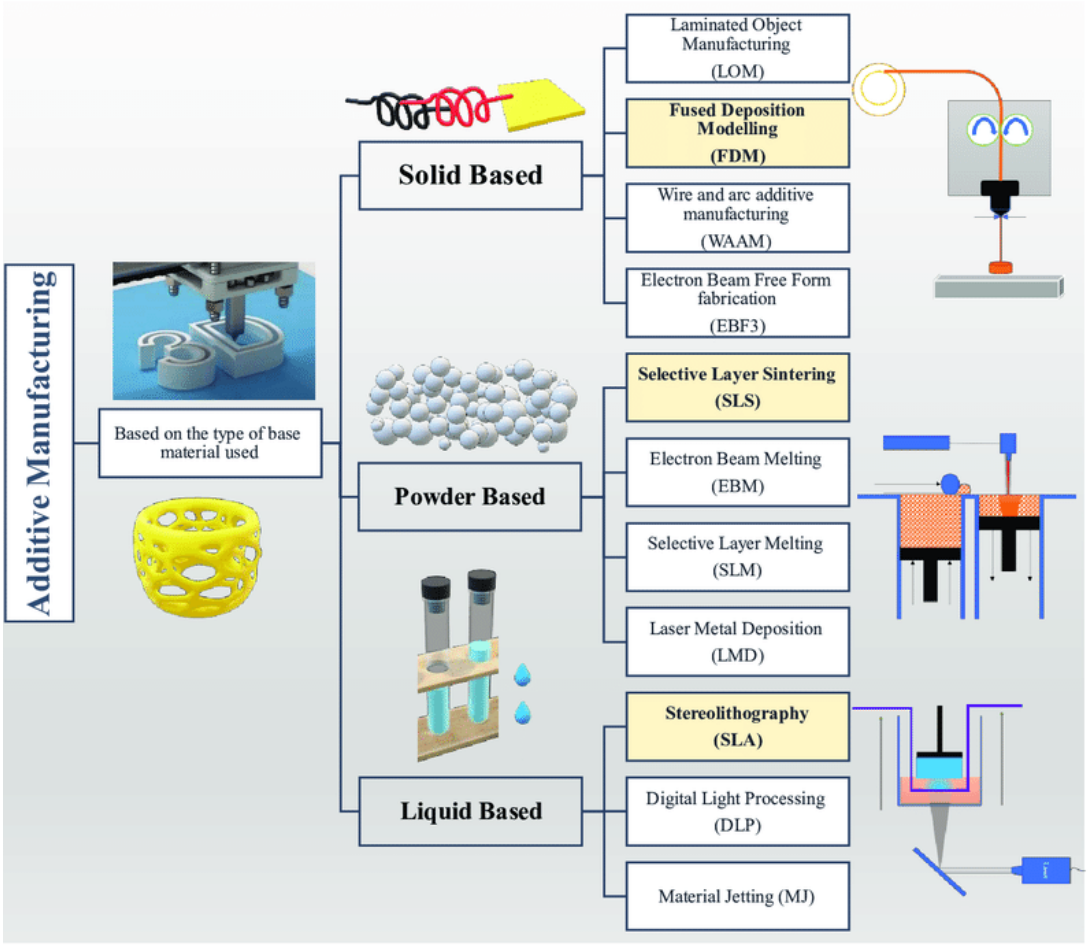

Figure 4 : Classification of AM methods based on the type of base materials (FDM, SLS, and SLA) [32]

and cost-effective prototyping capabilities, 3D printing has been widely employed by designers and architects to build both aesthetic and practical prototypes. It has been possible to reduce the cost of producing a product by using 3D printing. There have been several 3D printing applications in various sectors, from prototypes to finished items, throughout the last few years. Products customization and change in design have been a difficulty for producers due to high expenses. Despite this, AM is capable of creating small batches of customized items at a lower cost than traditional methods. In 2020, Wohlers Associates [33] estimated that half of all 3D printing will be used to produce

commercial items, and this trend is now taking hold. The increasing trend of utilizing the 3D manufacturing method over traditional approaches is ascribed to various benefits, such as the creation of complicated geometries with extreme accuracy, optimum material savings, versatility, and personal customization. It is possible to print using a wide range of materials including ceramics, metals, polymers, and concrete. When printing composites in 3D, the most common materials are polylactic acid (PLA) and acrylonitrile-butadiene-styrene (ABS) [34]. In order to receive the full benefits of 3D printing innovation, more research is required to identify and remove the barriers that prevent its widespread use. Tools for calculating the total cost of ownership, i.e. AM-oriented CAD solutions with improved user-friendliness and enhanced simulation features should be implemented. As a result of 3D printing's ability to mass customize products, each one may be unique while keeping a low price owing to the technology's mass manufacturing. AM has the potential for mass production of complicated geometries, such as lattice structures, where traditional techniques of manufacturing, such as casting are not easy and need more time-consuming tooling and post-processing. Machine design must be improved to boost fabrication speed and reduce costs. In addition, the AM application's higher prices and time-consuming nature continue to hinder mass manufacturing [35]. There are seven distinct processes from part design through part application in the standard additive manufacturing process shown in Figure 5. Orientation and positioning of parts can be done before or during machine setup, depending on the AM machine and software provider.

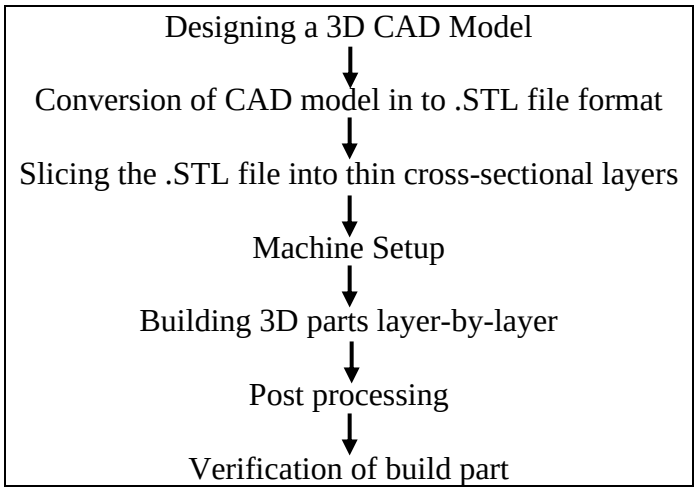

Figure 5: Basic steps in additive manufacturing [36]

2.2 3D-Printing Techniques:

In order to address the need for producing complicated designs with high qualities, different types of AM methods were developed. Fused deposition modeling is indeed the most popular 3D printing technique that is based on polymer filaments. Stereolithography, SLM, liquid binding in three-dimensional printing (3DP), SLS as well as LOM, inkjet printing, and direct energy deposition (DED) are the basic methods of AM. Each of these approaches is briefly described, their applicability and materials needed are presented, and their advantages and disadvantages are explored.

2.2.1 Fused Deposition Modelling:

FDM process utilizes a constant flow of thermoplastic polymer to 3D print layers of materials (Fig. 6). The material is heated to a semi-liquid condition at the nozzle before being extruded on to plate or over the layers that have already been printed. The ability of the polymeric fibers to harden at room temperature after printing is made possible by their thermo-plasticity, which is a critical attribute for this printing approach [37]. Mechanical weakness was discovered to be caused by inter-layer distortions. FDM's primary advantages are its low cost, rapid speed, and ease of use. Its principal shortcomings are poor mechanical qualities, layer-by-layer appearance and a restricted selection of thermoplastic materials [38]. The mechanical qualities of 3D printed items have been improved thanks to the development of fiber-reinforced composites made with FDM [39], [40].

2.2.2 Stereolithography (SLA):

SLA is a 3D printing method, often known as resin 3D printing, has grown in popularity due to its capacity to generate accurate, symmetric, and waterproof models and components in a variety of sophisticated materials with fine details and flawless surface texture. SLA is among the earliest technologies of additive manufacturing, which were introduced in 1986 [41]. SLA uses a chain reaction by shining an ultraviolet (UV) or electron beam on a resin or polymer liquid. When activated by UV light, the polymers (mostly acrylic or epoxy-based) transform into polymer chains immediately (radicalization).

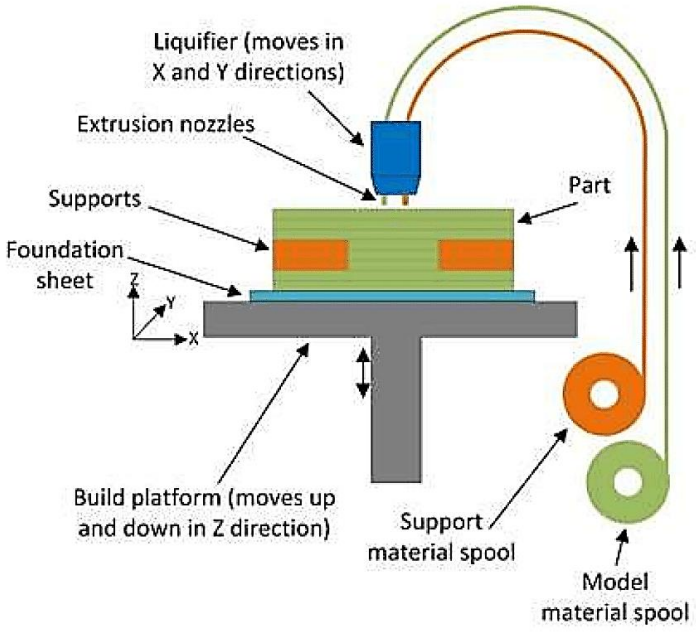

Figure 6: Schematic diagram of FDM printer [42]

For the following layers to be securely attached, a pattern is engraved into the resin layer after polymerization has taken place (Fig. 7). Afterwards, the resin that has not yet reacted is eliminated. Post-processing may be required for some printed items in order to get the correct mechanical properties. SLA can print with fine resolution as low as 10 nm [43], which produces high quality components. However, it is sluggish, costly, and limited in terms of the kind of materials that may be printed with it. In addition, the chemical kinetics and the process conditions are complicated. The thickness of each layer is determined mostly by the intensity of the light source and the length of exposure [41]. Additive manufacture of complicated nanocomposites may be done efficiently with SLA technology [44].

2.2.3 Powder bed fusion / Selective Laser Sintering (SLS):

In powder bed fusion procedures, fine powders particles are dispersed and compacted on a bed in a thin layer. With a laser beam or a binder, the particles in each layer are melted and bonded altogether. After a few layers of powder are rolled over each other and bonded together, the completed 3D component is created (Fig. 8). Additional treatment and details, such as coating or sintering, may be required once the powder has been removed. According to this approach, powder size dispersion and packaging, which

affects printing densities, are the most important aspects. With a low melting/sintering temperature, a liquid binder should instead be utilized for powders that are too hard to melt/sinter with the laser.

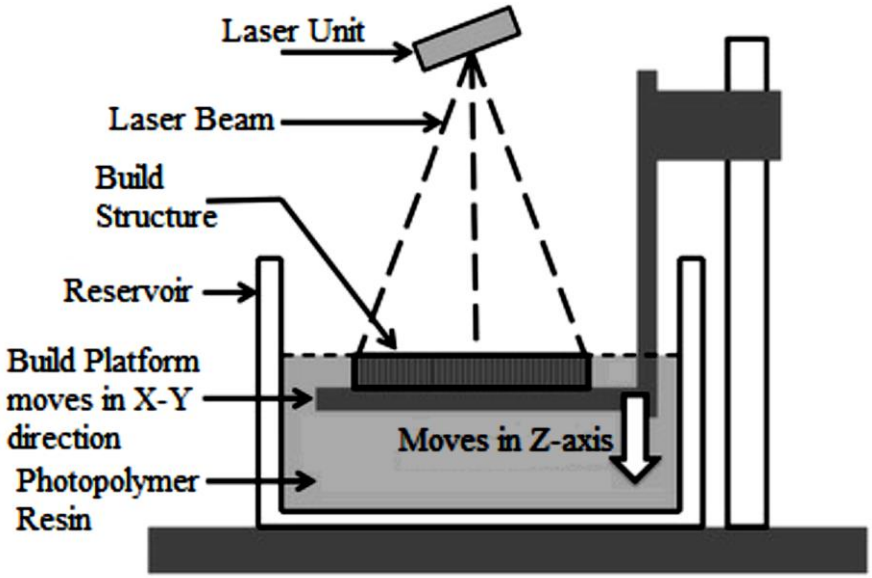

Figure 7: Schematic of SLA process [36]

Only some metals, such as aluminum and steel, are suitable for selective laser melting, while SLS may be used for a wide range of metals, alloy and polymers [45]. Because the powders aren't totally melted during SLS scanning, the higher local temperature on the grains' surfaces causes molecular fusion. As a consequence of a laser scan, the powders are thoroughly melted and bonded collectively, resulting in better mechanical characteristics.

An important factor in 3DP is the binder's chemical and rheological properties, as well as the shape and size of the powder particles. Parts printed by binder deposition have a higher porosity than parts printed by laser sintering or melting. The main parameters of sintering operation are laser power and scanning speed. Powder bed fusion has high resolution and print accuracy, making it more suitable for printing complicated shapes. This technique is extensively used in application areas like tissue engineering, lattices, aviation, and electronics. The main benefit of this method is that the powder bed acts as a foundation, easing the removal of supporting material. The main disadvantages of

powder bed fusion are significant expenses and high porosity when using a binder [43], [45].

2.2.4 Inkjet Printing:

AM of ceramics utilizes inkjet printing as a primary technology. Printing complicated and advanced ceramic structures like scaffolds is achieved with this technology. The injection nozzle is used to pump and deposit drops of a ceramic suspension, such as zirconium oxide powder mixed with water, onto the target [46].

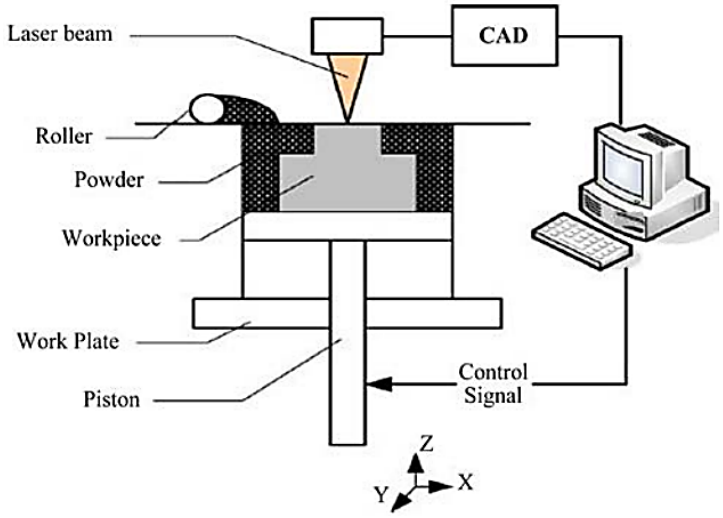

Figure 8 : Schematic diagram of SLS process [47]

After forming a pattern, the drops eventually harden enough to retain the next layer of printed material (Fig. 9). For complicated geometry, this technology is rapid and effective, making it easier to design and manufacture them. Ceramic inks come in two major forms: wax-based and liquid suspensions. In order to solidify the ink, melted wax-based ink is deposited on a cool substrate. There is a difference between the evaporation of liquid and solidification of solids in suspensions.

It is important to consider aspects such as ceramic particle size distribution, ink thickness and mineral composition, and print speed when determining the quality of inkjet-printed components [48]. This method's key limitations are its failure to manage flowability, fine resolution, and layer stickiness. Contour crafting, a printing technique comparable to inkjet printing, is the most common way of producing huge objects using additive manufacturing. Larger nozzles and high pressure can be used to extrude concrete paste or

dirt with this technique. A prototype of contour crafting for use in lunar architecture has been developed [49].

2.2.5 Laminated object manufacturing:

LOM was the first commercially successful additive manufacturing technique. LOM is dependent on slicing and laminating strips or reels of polymers layer-by-layer. When many layers are glued simultaneously, they are sliced accurately with a mechanical cutting tool or beam and afterwards reassembled.

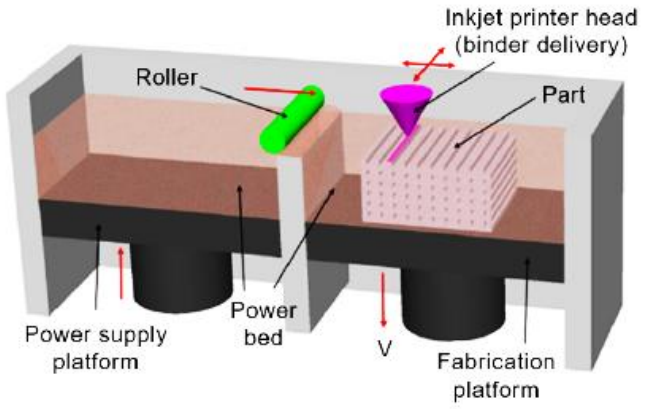

Figure 9: Schematic diagram of inkjet 3D printing [50]

In thermal bonding of ceramic materials and intermetallic, the form-then-bond process is particularly beneficial since it enables the development of interior details by eliminating surplus materials prior to binding. After cutting, the extra materials are retained for support, and they can be discarded and reused once the operation is complete [51]. Laminated object manufacturing can be used for different kind of materials like ceramics, metal-filled tapes, polymer composites and paper. In some cases, additional post-processing, like high temperature treatment, may be necessary.

2.2.6 Direct Energy Deposition:

Direct energy deposition is another additive manufacturing technology that equally combines material and heat. A plasma arc, electron beam or laser can be used as the heat source for DED technique while metal in powder form or wire is used as the raw ingredient for the final product. The coating efficiency of powders is lower than that of metal wire because only a fraction of the particle is heated and adhered to the substrate

[52]. A pressure chamber or vacuum is required for electron beam systems to work in DED, just like the E-PBF, but inert gases must be introduced in a different way.

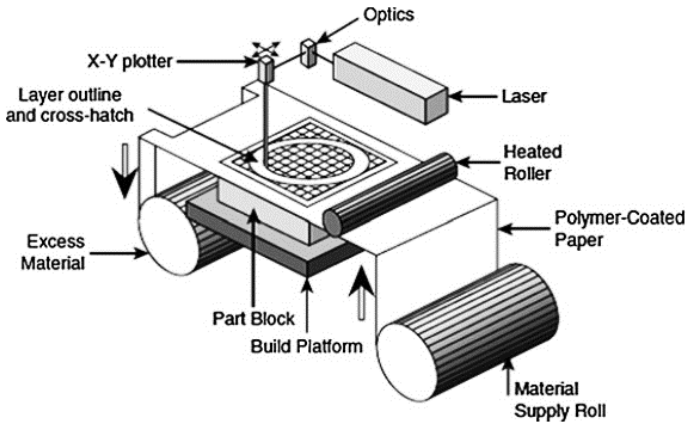

Figure 10: Schematic diagram of LOM process [51]

Inert gas is commonly pumped into the injectors of powdered DED equipment, shielding the molten area and decreasing oxidation [31]. When comparing to SLS or SLM, the precision of DED is 0.25 mm and surface texture is both poorer, and it can only make parts that are simpler in design. As a result, DED is frequently used to repair and replace big components with low computational complexity. In addition to saving money and time in the production process, DED offers good mechanical qualities and precise compositional stability. Turbine engines re-pairing and other specialist operations in the aerospace and automotive industries can benefit from this technology[51].

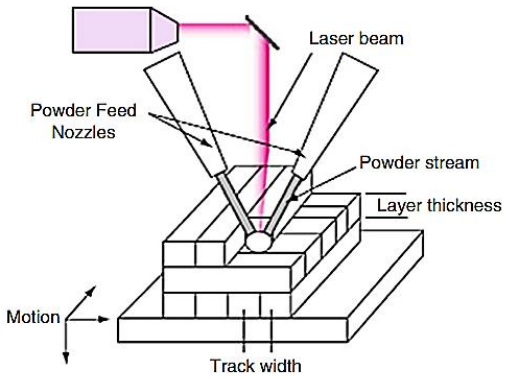

Figure 11: Schematic diagram of direct energy deposition [53]

Materials, uses, benefits, and limitations of different types of additive manufacturing techniques are summarized in Table 1:

Table 1: A summary of materials, application, benefits, and limitations of the main methods of additive manufacturing

Method	Materials	Applications	Benefits	Limitations	Resolution (um)
FDM	fiber-reinforced polymers, thermoplastic polymers	toys components composite parts	high speed low cost	Weak mechanical properties limitation in materials	50 µm to 200 µm [43]
Powder Bed Fusion (SLM, 3DP, SLS)	fine powder alloys ceramics polymers	aerospace electronics medical	high quality good resolution	slow speed porosity rate is higher expensive	80 µm to 250 µm [43]
Stereolithography (SLA)	resin with active monomers	prototyping biomedical	high quality fine resolution	limitation in materials layer to layer finish slow speed of printing	10 µm [43]
Inkjet Printing	concreate ceramics soil	buildings large structures biomedical	print large structure high print speed	coarse resolution requires maintenance lack of bonding	5 µm to 200 µm [54]
LOM	paper rolls of metals ceramics metal tapes	manufacturing of paper electronics small structures, foundry sector	less manufacturing time low cost	less accuracy limited in complex structure production	Depends on thickness
DED	powdered metals and alloys hybrid polymer-ceramics wire ceramics	biomedical aerospace retrofitting	less manufacturing cost and time good mechanical properties accuracy in composition	low accuracy less surface quality limitation in complex structures production	250 µm [51], [53]

2.3 3D Printing CAD Configuration

The selection of the right CAD software to transform a three - dimensional model into additive manufacturing format is the most critical phase in the 3D printing technique. Solid-works, CATIA, Blender, AUTOCAD, Pro-E, 3DS MAX and Fusion 360 are some of the most common software's used to convert CAD models into 3D printing format, The standard formats for transferring mathematical data of CAD model for 3D printing are STL, IGES, STEP and DXF as listed in table 2. To slice a 3D model into thin layers for fabrication, mostly STL format is adopted.

Table 2 : Commonly used slicing formats for 3D printing

Interface	Full Abbreviation
STL	Standard tessellation language
IGES	Initial graphic exchange specification
STEP	Standard for exchange of product data
DFX	Drawing exchange format

However, developing the geometrical design can be difficult because numerous aspects in the designed model can delay or even stop the 3D printing process. Tessellation is a process that converts a 3D CAD model into a triangular mesh model, which is used to create the object's exterior layers. It takes more effort and time to build a tessellated prototype which is more accurate in dimensions [55].

The common 3D printing softwares used nowadays are Cura, ZPRINT, Quickslice, Catalyst, Simplify 3D, XYZ Printing and Creality etc. These software are used to slice the 3D model into thin layers. The main purpose of these software is to define process parameters, i.e layer thickness, print speed, raster angle, layer height, shell thickness, infill patterns and infill density. The determination of process variables is closely related to the required materials, manufacturing cost, development time therefore this is highly critical phase and should be addressed with additional attention. The primary function of slicing software is to build 2D cross-sections of CAD geometry with straight lines to

make the shape of each layer regardless of any 3d printing techniques being utilized. The slicing process can be described in four steps as illustrated in the figure 12 [56].

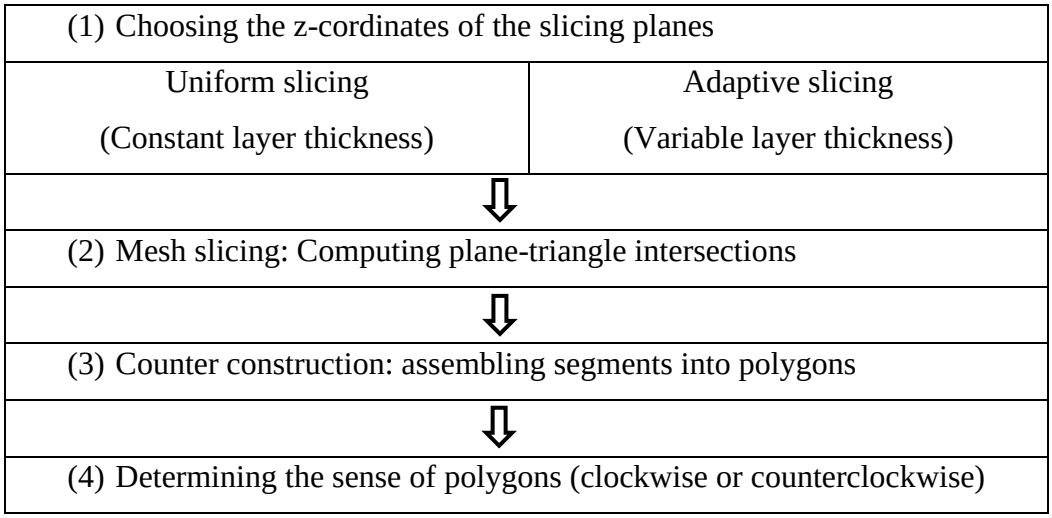

Figure 12: Steps of slicing CAD geometry [56]

Slicing software also generates support structures for a CAD geometry using a 3D printing software algorithm. However, based on the AM method, such as FDM, SLS, SL LOM, creating the supporting structure is not an integral step of the process. The data for polygonal ordering, support structures, standard orientations, is stored in the form of a file, which is then transferred to the 3D printing machine's language for additional processing Eventually, the component is constructed using layer by layer deposition, of the starting material.

2.4 Comparison of 3D Printable Material:

Additive manufacturing technologies are using a wide range of materials, from chocolate to complex multi-functional materials. Materials such as filaments, powder, wire, sheets, inks and pastes can be utilized in various additive manufacturing technologies. Polymers are the most prevalent materials produced for the sports, architecture, aerospace, medical, toy and automotive industries. Polymers are mostly utilized in 3D printing in the form of filaments in FDM which is the most popular technology, while auxiliary binders or powders are utilized in the powder-bed technology or resins in SLA. The most popular forms of polymers for 3D-printing are thermoplastic polymers like PLA, polymide, ABS, polycarbonate and different types of thermo-setting polymers such as polyamides,

photopolymer resin and polystyrene [5]. A summary of the main applications, advantages, and limitations of some of 3D printing materials is discussed in table 3.

Table 3: Summary of materials applications, advantages, and limitations used for 3D printing

Materials	Applications	Addvantages	Limitations
Polymers	medical sports automobile aerospace toy biomedical	cost effective fast prototyping complex geometries	weak mechanical properties limitation in polymer selection anisotropic mechanical properties
Metals & Alloys	automobile aerospace biomedical army	multi-function optimization mass-customization less material waste less assembly components easy to repair damaged metal parts	limitation in alloy selection bad surface finish inaccuracy in dimension processing may be needed after finishing
Ceramics	chemical sector aerospace automobile biomedical	low porosity of lattices complex geometries like scaffolds for human organs, low fabrication time good control on composition and microstructure	limitation in 3D-printable ceramics selection inaccuracy in dimensions bad surface finish processing required after production
Concrete	construction and infrastructure	mass-customisation Less labour needed Useful in harsh environment	appearance of layers after printing poor layer adhesion, anisotropic mechanical properties difficulties in construction of larger structures limitations in printing techniques

2.5 Scanning Electron Microscopy:

SEM uses a concentrated electron laser to inspect the surface of a specimen to generate structural images. Electrons come into contact with atoms through the specimen, generating a wide range of signals which includes details regarding the specimen's surface characteristics and morphology [57]. Since the invention of SEM in

1926 [58], it has been an essential part of the research, making considerable contributions in medicine, biology, and engineering materials field. Scanning electron microscope capture the images of specimen at higher magnification up-to 10,000x [59]. The basic framework of SEM includes an anode, scanning coils, detectors, electron gun, electro-magnetic lens and a specimen holder.

Electrons are generated near the upper end of the section and accelerated to travel through a sequence of electromagnetic lenses to produce a focused laser of electrons that impacts the specimen's top surface (fig 13) [60]. The sample is placed on a sample holder within the chamber region, and the microscope is operated at low vacuum, with both the column and the chamber evacuated by means of vacuum pump. The suction level is dictated by the design of the microscope. The position of the electron beam on the sample is controlled by scanning coils situated directly above the objective lens. These coils allow electron beam to be traced over the surface of the material. Electron beam scanning allows data about a specified location on the material to be captured. As a consequence of the electron sample interaction, a plethora of signals are generated. Sensors are then used to quantify those signals [60].

2.5.1 Interaction between Specimen & Electron Beam:

SEM creates high-resolution images while examining the material with the electron gun. Electric charges, back-scattered charged particles, and distinctive X-rays are produced as the electron interacts with the material. Several detectors capture those impulses to produce images, that are subsequently seen on the computer display. As the beam of electrons strikes the specimen's surface, it penetrates to a depth of a few microns, based on the applied potential voltage and density of the specimen. As a result of this contact within the specimen, several signals, such as backscattered electrons and X-rays, are generated (see Figure 14) [60]. A variety of factors, such as the diameter of the electron beam and the volume of the beam's contact with the sample, influence the highest resolution achieved in a SEM. Although it is capable of approaching to particle’s precision, certain SEMs may obtain resolutions of less than 1 nm. Nowadays, SEM’s typically resolution varies from 1 to 20 nm, however workstation devices generally have a resolution of 20 nm. [61].

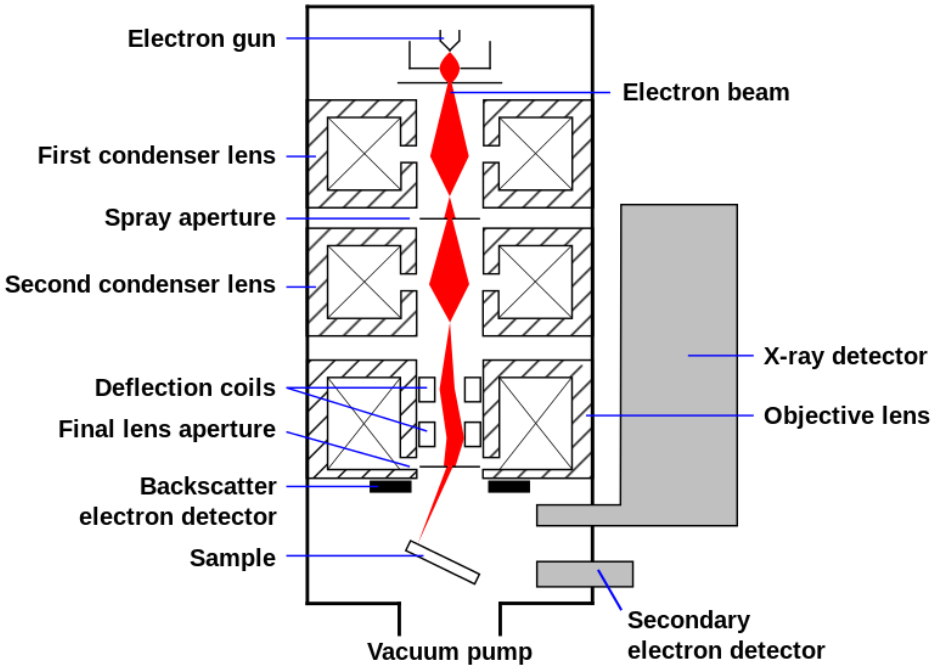

Figure 13: Schematic diagram of the SEM build structure [60]

2.5.2 Sample preparation for SEM:

A beam of electrons is directed straight down a series of objective lenses inside a highly vacuumed chamber by an electron emitter at the head of the microscope. The lenses are housed in a highly vacuumed chamber to prevent ionization and contaminating the sample from extraneous particulates. These lenses aid in directing the electrons onto the specimen. The electron sample interaction is then transformed to a 3D representation of the material that is computationally produced. SEM specimens must be conductive or, at the very least, its surface should be. This is due to the fact that non-conductive objects collect electrons on to their surfaces. Image artifacts result from the accumulation of charge on to the sample surface. As a result of their natural ability to conduct an electric current, metallic specimens need no extra processing. Non-metal specimens, on the other hand, must be coated with a conducting substance during SEM specimen preparation in order to be SEM compatible. A thin coating of gold is generally adequate. The conducting substance is deposited onto the specimen using a device known as a sputter coater [62]. Before inserting sample in SEM machine, evaluate the specimen's

dimensions, geometry, condition, and conducting ability. The smallest possible samples size should be used whenever possible. The detection range of the microscope is up to 1 µm from the sample surface. It is important to consider critical aspects of sample cleaning, drying, mounting and storage before initiating the imaging process [63].

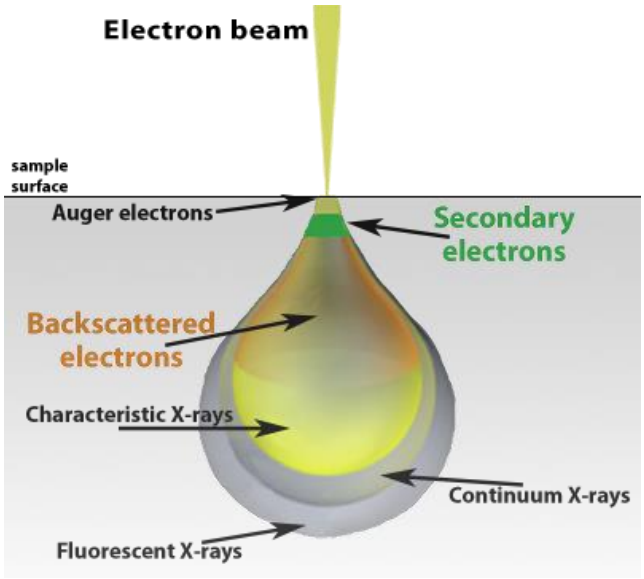

Figure 14: Schematic diagram of Electron beam and specimen interaction [60]

2.6 Research Gap:

In the light of the literature review of published articles, following aspect was identified, which proved to be very helpful in the present study. Earlier researchers focused either on a single process variable or a single material at a time. For instance Khan et al. (2005) [64] as well as Sood et al. (2010) [65] reported that the tensile modulus of 3D printed components deteriorated with the increase in layer thickness. There is little existing literature on the effect of multiple design (material/geometry) variable on the performance of everyday use applications. For better understanding on the effective utilization of 3D printing process, it is essential to investigate the impact of multiple design (material/geometry) variables on the behavior of final product.

Thereby in the present study an explicit dynamic module was used to investigate the impact strength of a customized hair clipper comb developed using two different thermoplastics (PLA/ABS) and two different infill percentages (solid model and shell model).

CHAPTER 3

MATERIALS AND METHODOLOGY

3.1 Introduction:

In this chapter, methodology of the whole study is discussed. The chapter is divided into 4 sections including 3D modelling, numerical analysis, 3D printing and characterization. This work presents, the impact strength of a hair clipper comb under the drop case. Designed components was subjected under numerical analysis using explicit dynamics module in ANSYS (version 17.2). More precisely, the stress distribution of the designed model was investigated by dropping it from a height of 5ft at different angles. Then the sample were fabricated using FDM and surface morphology was analyzed by SEM.

3.2 3D Modelling:

A 3D solid body model and a shell model of the product were created on CAD software ONSHAPE. The component was designed based on dimensions from an actual commercial product and a shell having thickness of 1 mm was introduced in a designed model. The volume of the solid body model is $9.37 \times 10^{-6}\text{m}^3$ and the volume of the shell body model is $6.72 \times 10^{-6}\text{m}^3$. The solid and shell models are shown in Figure 15 (a-c).

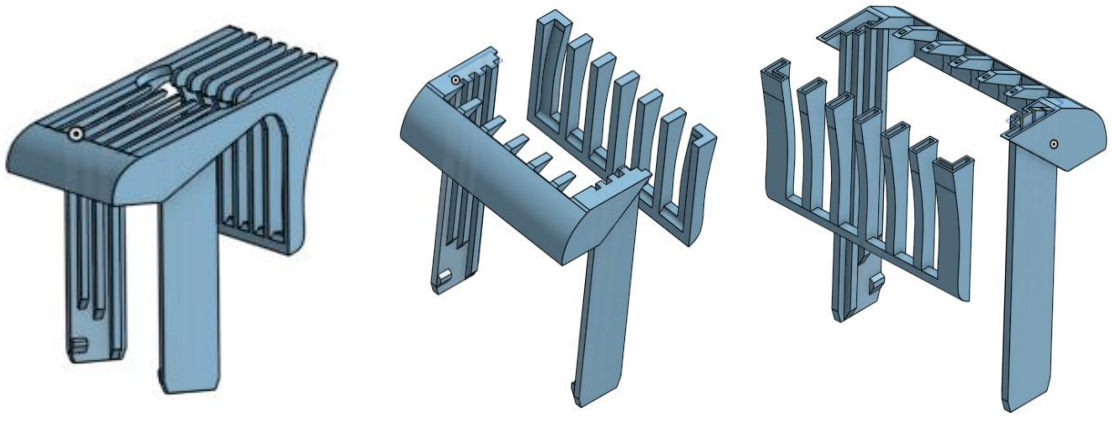

(a) (b) (c)

Figure 15: 3D model of hair clipper comb: (a) full model: (b) cut model of solid design: (c) cut model of shell design

3.3 Finite Element Analysis:

FEA simulation is extensively used for the analysis of designed components under various loading conditions to minimize experimental testing. In this work the designed model was exported from ONSHAPE to FEA software ANSYS. The free fall motion (drop test) of customized hair clipper comb as a non-rigid object was investigated using explicit dynamics analysis on ANSYS.

3.3.1 Meshing

After designing the geometric model, mesh generation was performed, the software divides the model into small elements connected on a common point called nodes. The mesh details are given below in Table 2 and Fig 16 shows the mesh elements and nodes.

Table 4: Mesh details

Model	Solid Body	Shell Body
Mesh type	Solid Mesh	Solid Mesh
Mesh quality	High	High
Element size	0.62 mm	0.62 mm
Total elements	350734	192986
Total nodes	77024	63122

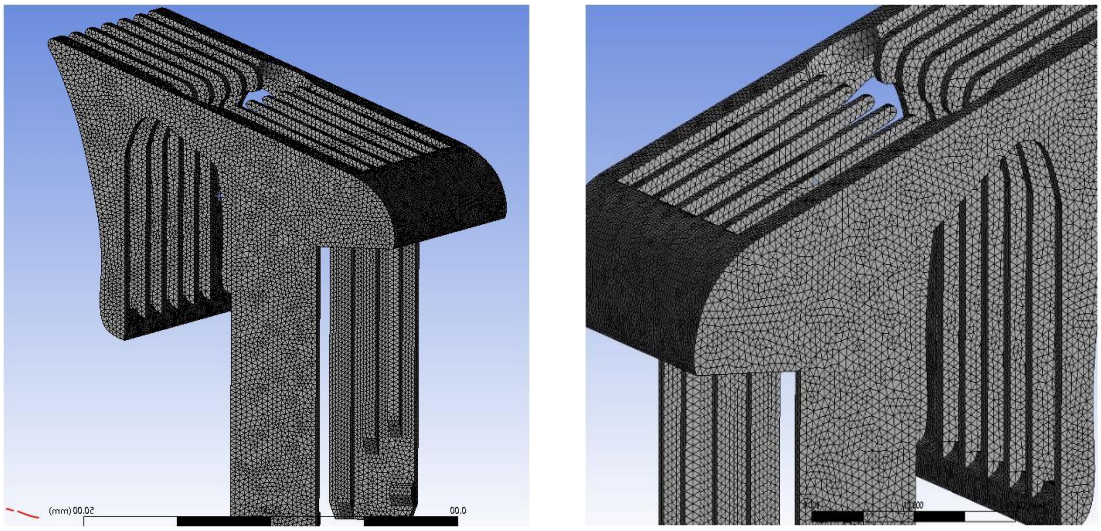

(a) (b)

Figure 16: Meshing: (a) mesh applied on full design: (b) meshing zoomed view

Mesh convergence analysis was performed manually using different mesh sizes to compute the results and comparing the calculated von mises stresses. From the results

shown in Figure 17 the stresses converge from mesh size 0.54 mm to 0.62 mm. So, 0.62 mm mesh size was selected. According to Mesh Metric developed by Ansys, Inc [66], mesh quality factor is important in terms of reliability of the results. High skewness values or low orthogonal quality are not recommended from scale in figure 18 & 19. Generally, we need to keep minimum orthogonal quality >0.15, or maximum skewness <0.94. However, these values may vary depending on the location and physics of the cell. Skewness mesh metrics spectrum and orthogonal quality mesh metrics spectrum are given in Figs. 18 and 19 [67]. In our analysis results, average skewness value was calculated as 0.231 in Fig. 20 (a). According to Fig. 18, this value is excellent (0–0.25). Average orthogonal quality value was also calculated as 0.767 in Fig. 21 (a). According to Fig. 19, this value is very good (0.70–0.95).

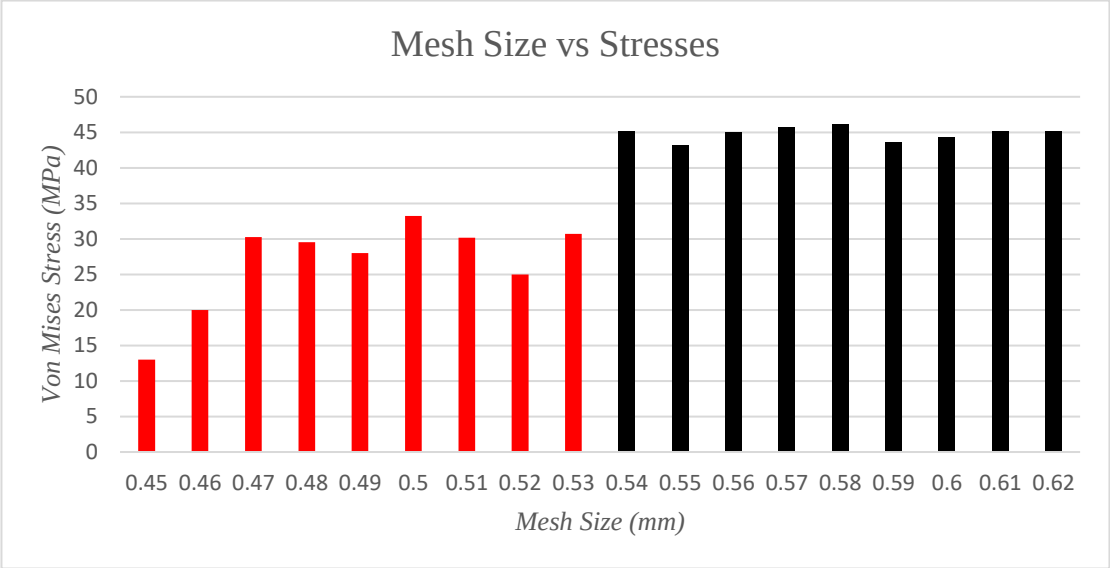

Figure 17: Mesh convergence analysis

Excellent	Very good	Good	Acceptable	Bad	Unacceptable
0-0.25	0.25-0.50	0.50-0.80	0.80-0.94	0.95-0.97	0.98-1.00

Figure 18: Skewness mesh metrics spectrum

Unacceptable	Bad	Acceptable	Good	Very good	Excellent
0-0.001	0.001-0.14	0.15-0.20	0.20-0.69	0.70-0.95	0.95-1.00

Figure 19: Orthogonal quality mesh metrics spectrum

Sizing	
Quality	
Check Mesh Quality	Yes, Errors
☐ Target Quality	Default (0.050000)
Smoothing	High
Mesh Metric	Skewness
☐ Min	1.3057e-010
☐ Max	0.98953
☐ Average	0.23144
☐ Standard Deviation	0.12744

(a)

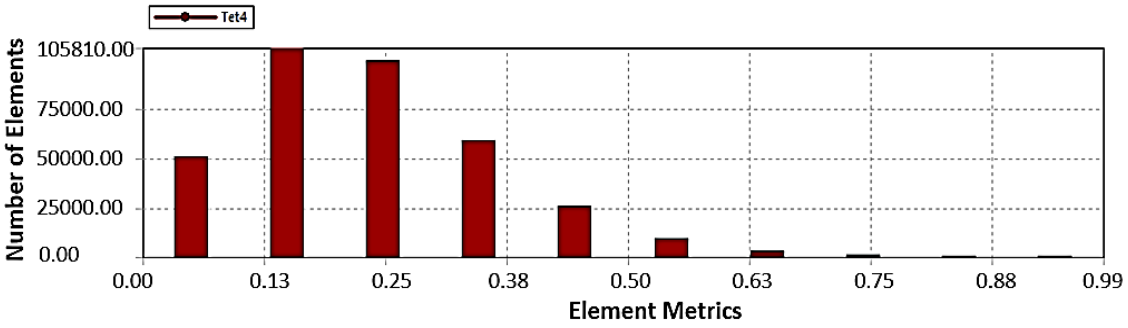

(b)

Figure 20: (a) Calculated average skewness value; (b) graph presentation of skewness

Sizing	
Quality	
Check Mesh Quality	Yes, Errors
☐ Target Quality	Default (0.050000)
Smoothing	High
Mesh Metric	Orthogonal Quality
☐ Min	1.0466e-002
☐ Max	1.
☐ Average	0.76719
☐ Standard Deviation	0.12575

(a)

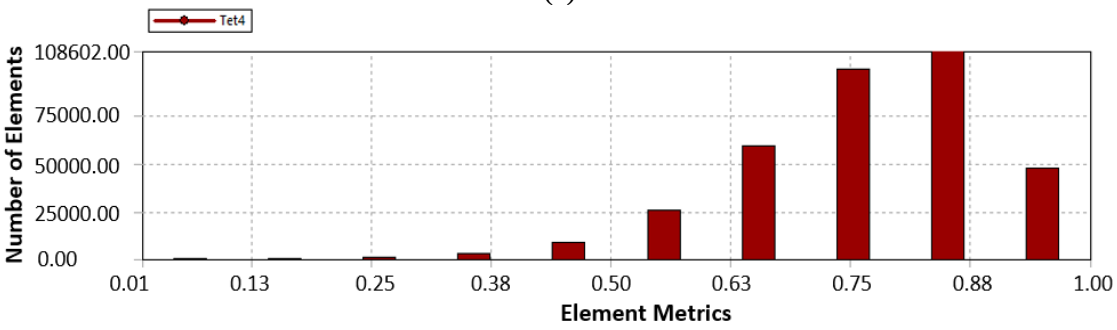

(b)

Figure 21: (a) Calculated average orthogonal quality value; (b) graph presentation of orthogonality

3.3.2 Material Selection:

The polymeric materials used for the drop test analysis were Acrylonitrile butadiene styrene (ABS) and Polylactic acid (PLA) to investigate the impact stress distribution on the designed model by dropping it from 5ft heights at different angles. Material properties are selected as per the ASTM D638. The important material properties are given in table 5 [68]–[71].

Table 5: Material properties

Material	**PLA**		**ABS**	
Model	**Solid Body**	**Shell Body**	**Solid Body**	**Shell Body**
Mass (g)	11.71 g	8.40 g	9.74 g	6.99 g
Mass density (kg.m^-3)	1250		1040	
Tensile Strength (MPa)	54.1		41.4	
Ultimate Tensile Strength (MPa)	59.2		44.3	
Young's Modulus (MPa)	3450		2390	
Poisson's ratio	0.39		0.399	

3.3.3 Analysis Setup:

The next step after meshing and material selection is to setup the drop test settings by manually setting the drop height, the orientation of drop plan. In the study the model was dropped from the height of 5 ft while subjected to gravitational pull. The model was dropped from two different orientations specified in figure 22. The software calculates the velocity of model at the moment of impact with ground from Eqn (1)

$$v = \sqrt{2gh} \tag{1}$$

where h is the height (m) and g is the gravitational acceleration (ms^{-2}). ANSYS use the explicit time integration to solve the drop test analysis which automatically calculates the response starting from the moment of impact.

3.4 3D-Printing:

Creality Ender-3 printer that operates on the principal of FDM technique was used to fabricate the designed part. The 3D printing machine setup is shown in Figure 23. Wide range of materials such as PLA, ABS etc can be used to print any designed part with accuracy and customized settings. The printing parameters for Creality Ender-3 printer are given in Table 6.

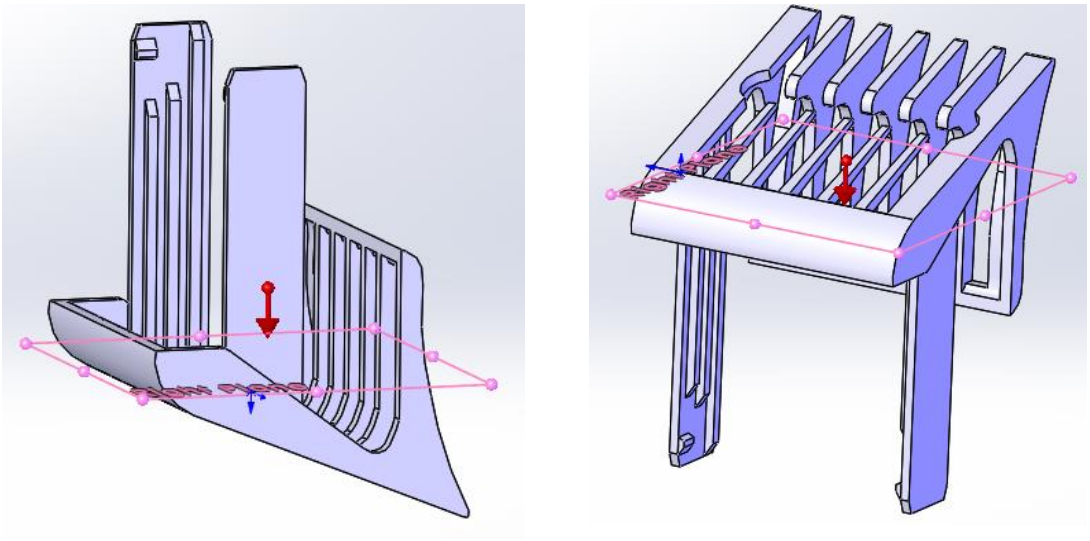

(a) (b)

Figure 22: Orientations for drop test analysis: (a) head drop: (b) leg drop

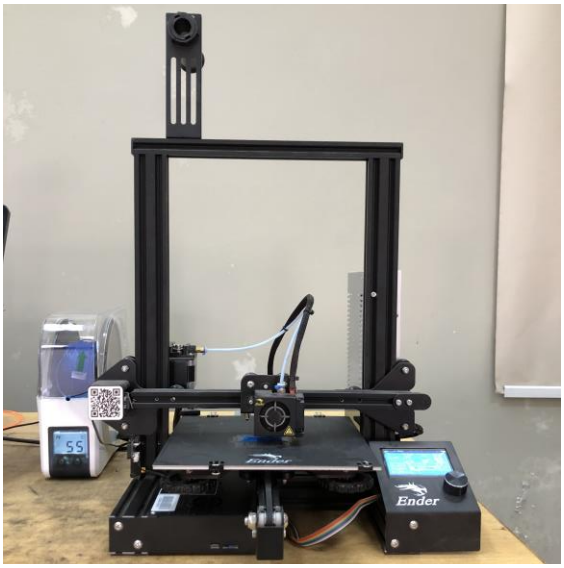

Figure 23: Creality Ender-3, 3D Printer

Table 6: 3D printer specifications

Fixed FDM parameters		
3D Printer	Creality Ender-3	
Material Used	PLA	ABS
Bed Temperature	60 °C	100 °C
Nozzle Temperature	210 °C	240 °C
Layer Height	0.2 mm	
Infill Density	100 %	
Print Speed	120 mm/s	
Slicing Software	Creality 3D	
Nozzle Diameter	0.4 mm	

A total of 4 samples (two solid samples and two shell samples for PLA and ABS) were fabricated using this setup. These samples are shown in Figure 12 below.

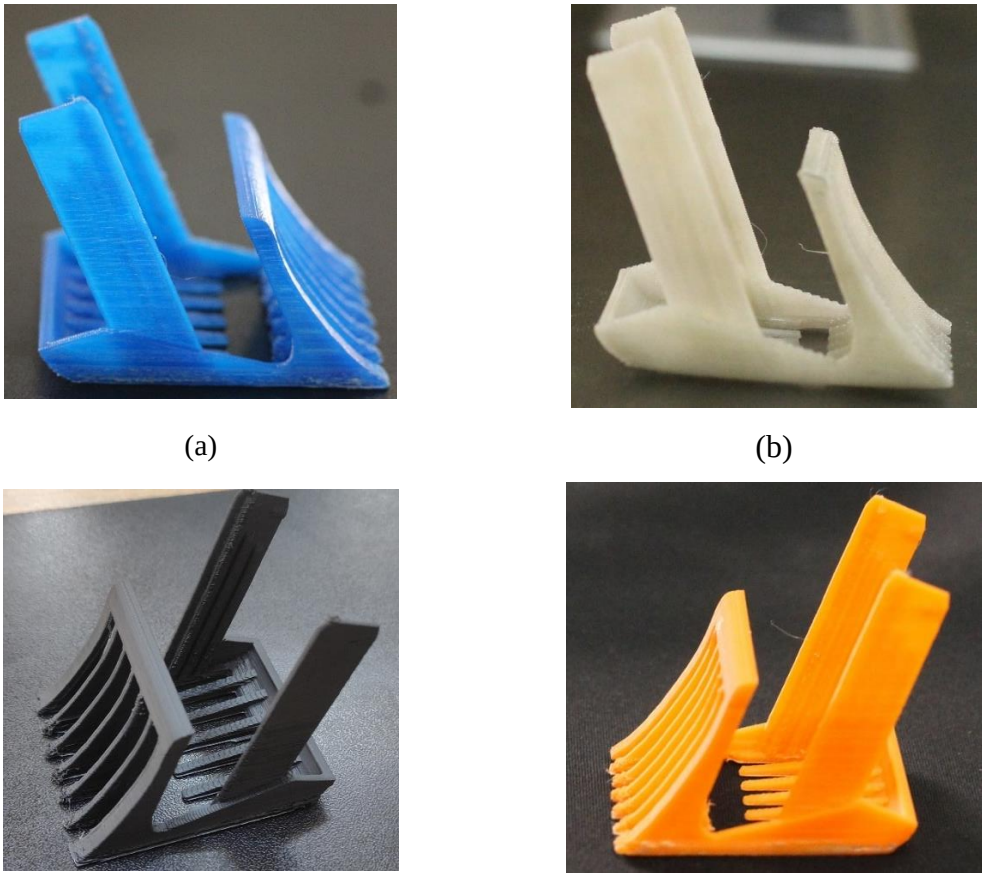

(a) (b)

(c) (d)

Figure 24: 3D printed samples: (a) PLA solid: (b) PLA shell: (c) ABS solid: (d) ABS shell

3.5 Scanning Electron Microscopy:

The strength of any material is directly linked to its microstructure. Therefore, the examination of microstructure of the cracked or fractured surface is very important to understand the reason of failure in material. In this study, the fractured surfaces of the hair clipper comb after drop test was analyzed. Furthermore, the external surface of 3D printed hair clipper comb was also examined to identify any defect formed during 3D printing. SEM was used at an accelerating voltage of 5 KV in the high vacuum atmosphere to examine the microstructure of fractured surface and as printed surfaces of the sample. The samples were carefully prepared for SEM analysis. The thin layer of gold was coated in a vacuum chamber to prevent the charging effect on the surface. This thin layer coating is significant as it provides a homogeneous surface for examination and clear SEM images [72], [73].

Chapter 4

Results and Discussions

4.1 Drop test analysis of the PLA model

First the Finite Element Analysis of the designed hair clipper comb was carried out to check the maximum strength with different material selection in head and leg impact using ANSYS. The 3D printed hair clipper comb was then dropped on the floor to validate the results from FEA. Figure 25 (a-b) shows stress distribution on hair clipper comb for the PLA solid model under head and leg drop. Results show that the maximum stresses are generated along the corner and middle of fins as shown in the enlarged views. The maximum stresses were found for Figure 25 (a) & (b) to be 60.4 MPa and 56.4 MPa respectively. These stress values are greater than the ultimate tensile strength (UTS) of PLA (59.1 MPa) [68].

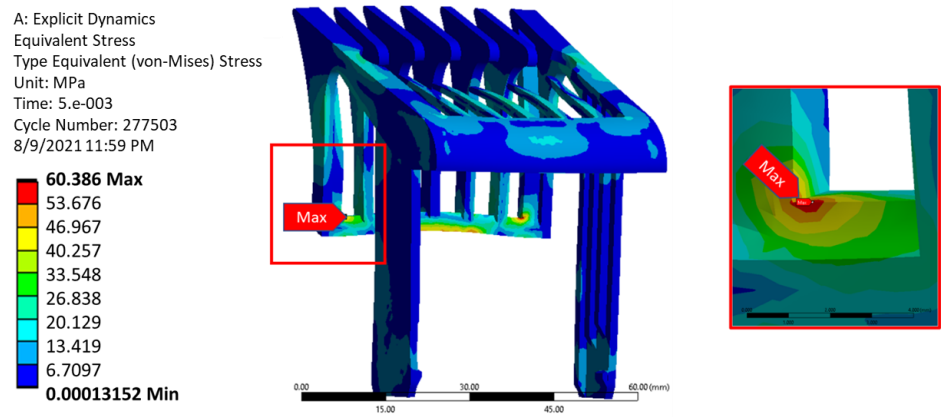

(a)

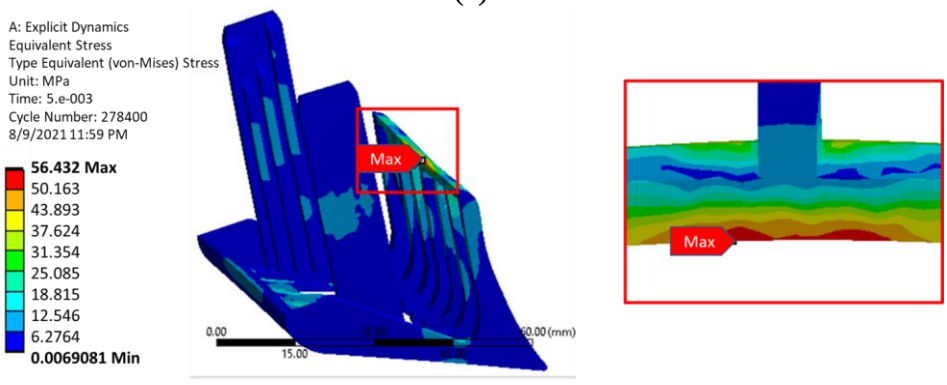

(b)

Figure 25: Solid body PLA simulation result: (a) stress distribution while leg drop: (b) stress distribution while head drop

After the solid model, a modified 1 mm shell model was created. Figure 26 shows stress distribution on shell model under head and leg drop test using the same material. The result shows that the maximum stress concentration was at the centre and sides of the hair clipper comb as highlighted in the enlarged view. The maximum stress values were 40.3 MPa and 30.9 MPa for Figure 26 (a) and (b) respectively. The maximum stress value for hollow design (shell model) in both cases is less than the UTS of PLA. The results point to the suitability of the shell model made of PLA material for hair clipper comb.

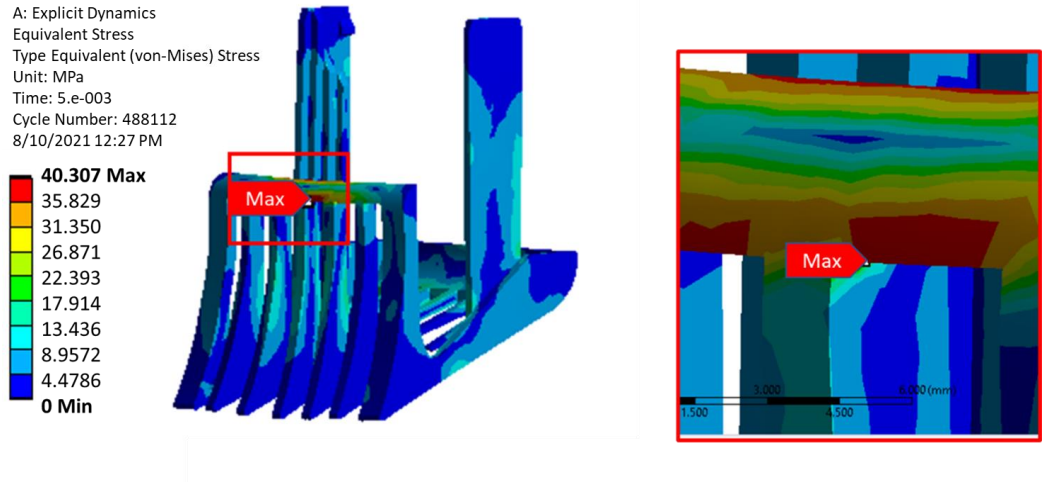

(a)

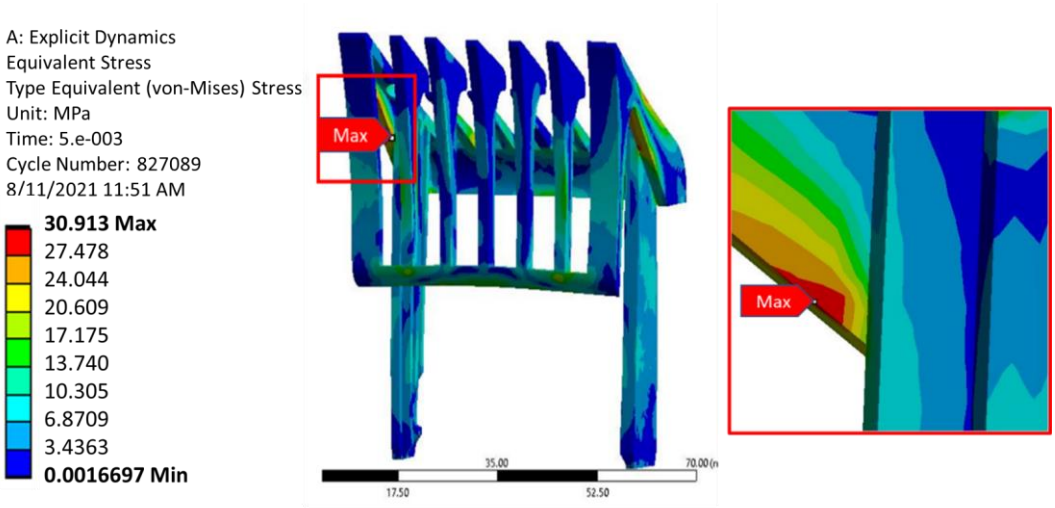

(b)

Figure 26: Shell body PLA simulation result: (a) stress distribution while head drop: (b) stress distribution while leg drop

4.2 Drop test analysis of the ABS model:

Figure 27 shows the stress distribution resulting from the free fall drop test for the solid model made of ABS. The stresses generated on the front face and in the corner of the hair clipper comb are highlighted in Figure 27 (a) & (b) respectively. The maximum stresses are found to be 42.8 MPa and 34.3 MPa respectively. These values are less than the UTS of ABS (44.2 MPa).

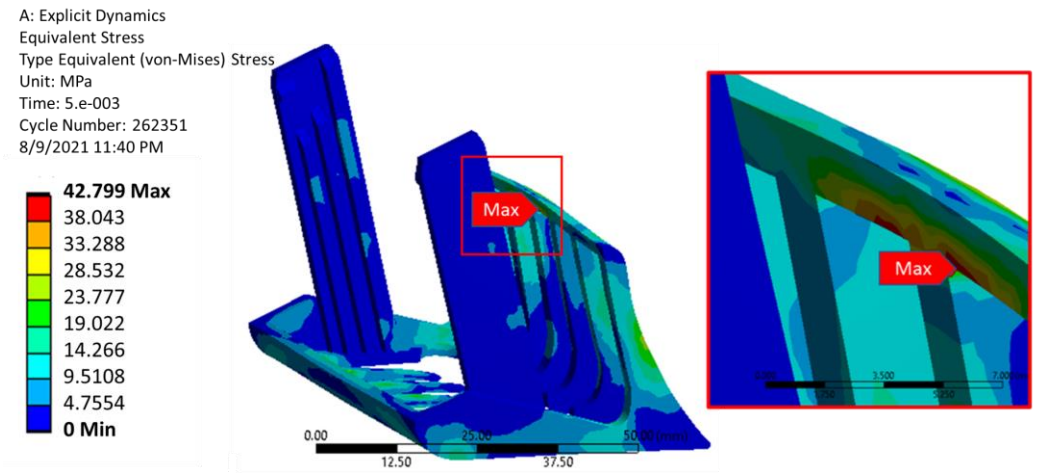

(a)

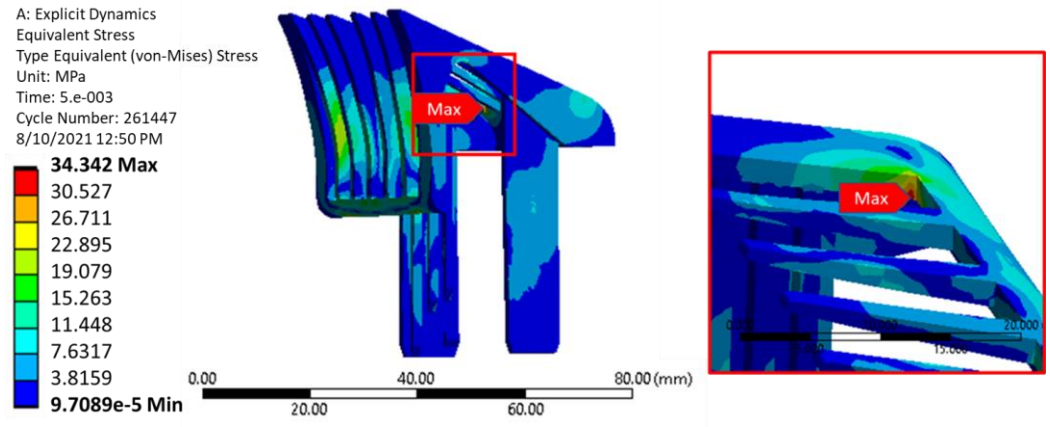

(b)

Figure 27: Solid body ABS simulation result: (a) Stress distribution while head drop: (b) Stress distribution while leg drop

Figure 28 (a) and (b) show the stress distribution on the shell model with the leg and head drop tests respectively. The maximum stresses are generated on the front face, having stress values 30.6 MPa and 26.9 MPa respectively. These values are also less than

the UTS of ABS. This means that ABS is suitable for impact in both solid and shell models. Table 7 summarizes the stress values from numerical analyses for all the cases.

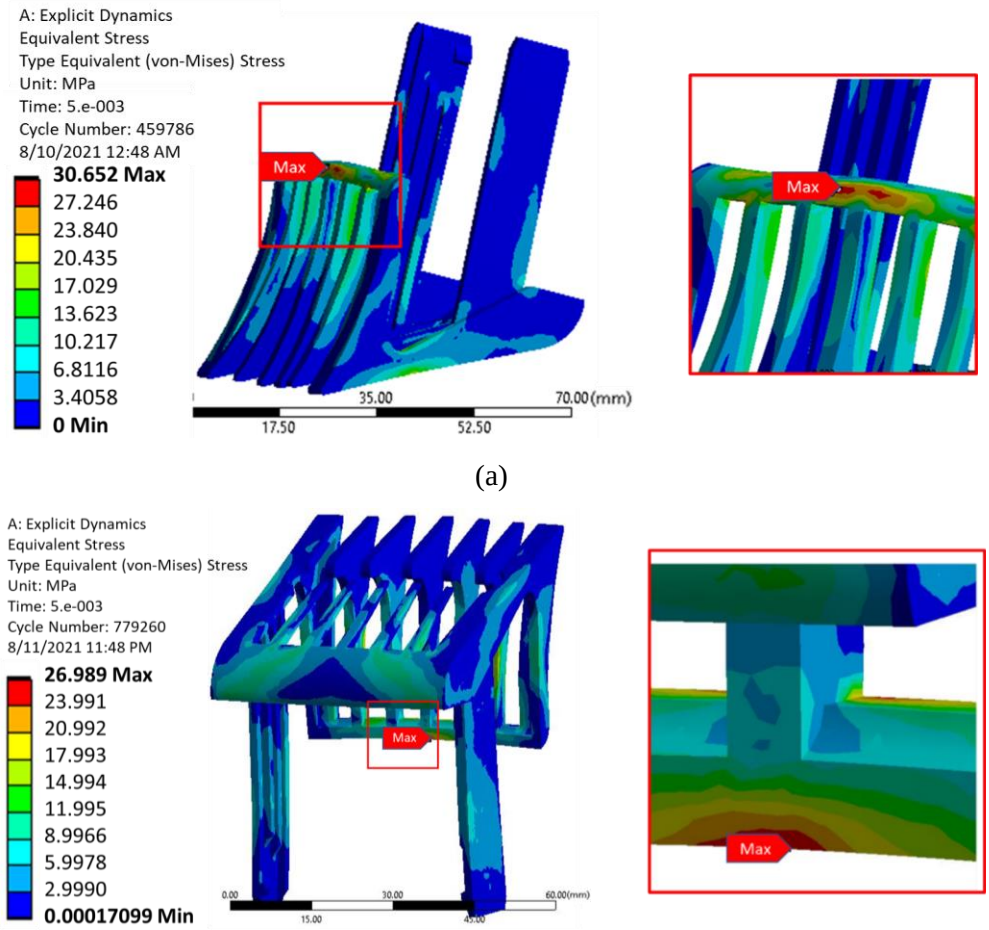

Figure 28: Shell body ABS simulation result: (a) Stress distribution while head drop: (b) Stress distribution while leg drop:

Table 7. Stress distribution on all design

Material	Maximum Stress Solid Model (MPa)		Maximum Stress Shell Model (MPa)	
	Head Drop	Leg Drop	Head Drop	Leg Drop
PLA	56.4	60.4	40.3	30.9
ABS	42.8	34.3	30.6	26.9

4.3 Drop test of 3D printed PLA & ABS Model

3D printed solid and shell models were dropped from the height of 5ft for validation of numerical results obtained earlier. Figure 29 (a-c) shows the manual drop test of 3D

printed customized hair clipper combs made of PLA and ABS. A crack originated in 3D printed PLA solid model after the impact. The crack originated exactly from the area where stress concentration was found to be maximum in the numerical simulation. This can be seen by comparing the highlighted area in Figure 29 (c) with that in Figure 25 (a).

(a) (b) (c)

Figure 29: Drop of 3D printed samples: (a) leg drop: (b) head drop: (c) crack originates in solid PLA model

4.4 Scanning Electron Microscopy

Fracture surface morphology of solid PLA model and ABS solid model in as-printed condition were analyzed using Scanning Electron Microscopy. SEM micrographs of fractured PLA and 3D printed ABS are shown in Figure 30 (a) and (b), respectively.

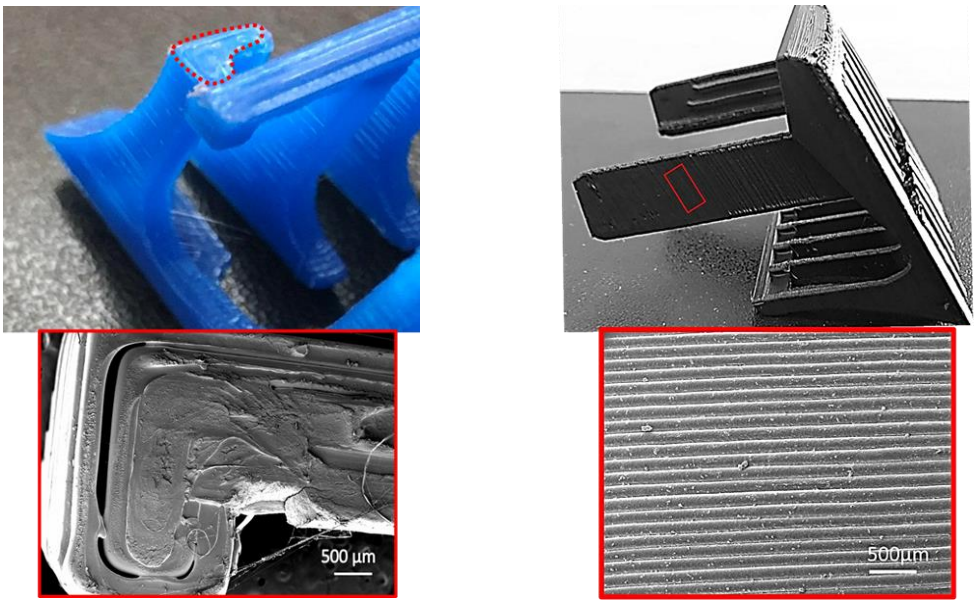

(a) (b)

Figure 30: SEM images: (a) neat surface of ABS 3D printed part: (b) fracture surface PLA 3D printed part

4.5 SEM of fractured PLA

Figure 31 shows that the extruded fiber string roughly 0.3 mm matches with the diameter of the extruder nozzle. The region encompassing surface morphology of single fiber selected for examination at higher magnification is highlighted in the red box. The central region of the surface of single fiber showing a relatively rough patch stretching over a span of about 100μm was in turn examined at a higher magnification as highlighted bt in the green box. Obvious signs of porosity perpendicular to the direction of extrusion were visible. Non-homogenous surface finish, bulging out of the PLA filament and corresponding porosity indicates defects induced during the manufacturing of the filament.

The region outlined in yellow doted line in figure 31 clearly represents poor adhesion between the subsequently printed fibers within the same layer. The interfacial bonding between neighboring filament passes starts when the interface temperature is above the glass transition temperature, which allows easy flow of the polymer material. The heated interface allows for diffusion to take place at the point of contact between neighboring filament passes during the 3D printing of polymeric materials via FDM, the semi-melted polymer is directed out of the nozzle at a temperature which is above its glass transition temperature. This filament gets deposited next to the previously deposited pass which is at a considerably lower temperature. Thereby, the interface temperature rises momentarily and then falls below the glass transition temperature, resulting in poor adhesion between neighboring filaments, which promotes the formation of voids and defects. A long internal void as seen at the exterior end of the part (outlined in yellow) is associated with the lack of temperature dependent interfacial diffusion/bonding as well as stresses associated with the sharp geometric corners prohibiting maximum interfacial contact.

The sharp corner region of stress concentration as observed in the impact test simulation, indicating internal fibre failure (highlighted in orange) is shown in Figure 31 (a). Inner region of single fiber shows a through crack originating from the exterior surface (region of high stress). The fractured surface region was further examined at higher magnification to analyze the presence of any internal defects as shown in the enlarged view in the green box. There are obvious signs of uniformly spread internal porosity with

a flat fracture surface indicating brittle fracture triggered by high stress and facilitated by the internal defects within the PLA filament.

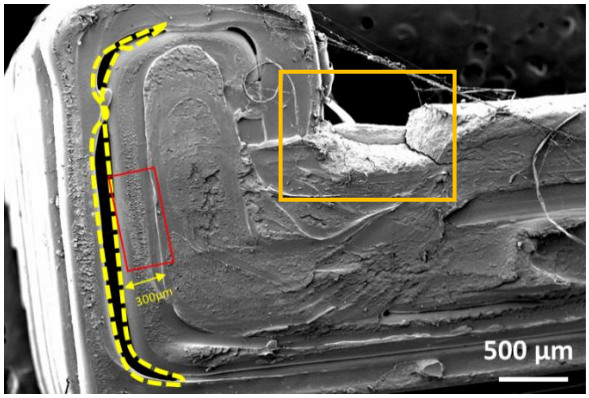

(a)

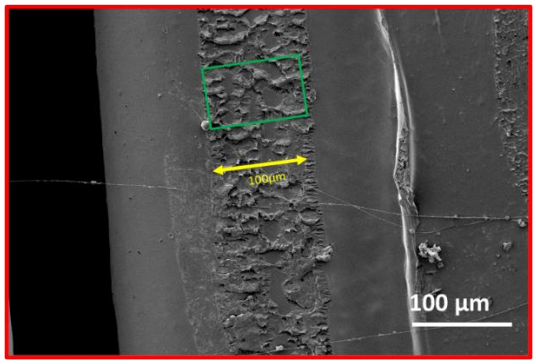

(b)

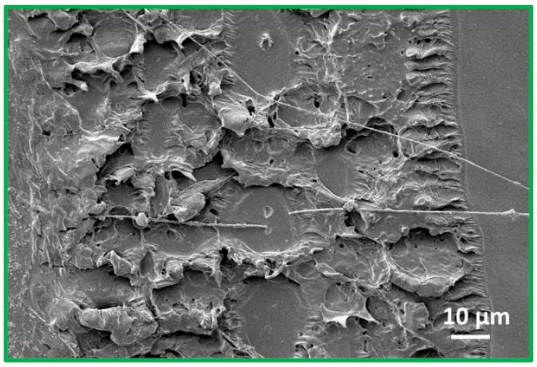

(c)

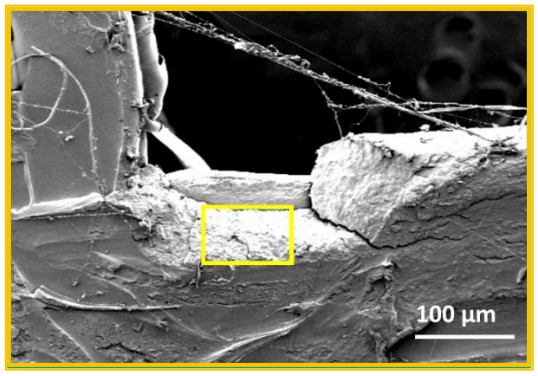

(d)

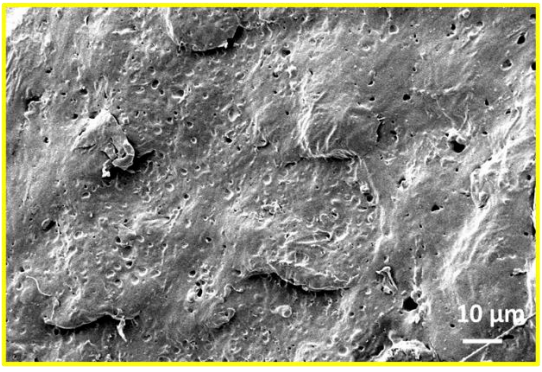

(e)

Figure 31: SEM image acquired from the fractured surface of impact tested PLA sample

4.6 SEM of as printed ABS

Figure 33 show the SEM images of as printed ABS. Visible signs of interfacial porosity suggest weak bonding between the fiber layers. SEM images clearly indicate that

interfacial bonding between neighboring filament is weak which was also the case with the PLA filament. The interface temperature is above the glass transition temperature here as well, which allows filament an easy flow while printing. The filament gets deposited next to the previously deposited layer whose temperature has in the meanwhile dropped, which results in poor bonding between neighboring filaments and promotes the formation of voids and defects.

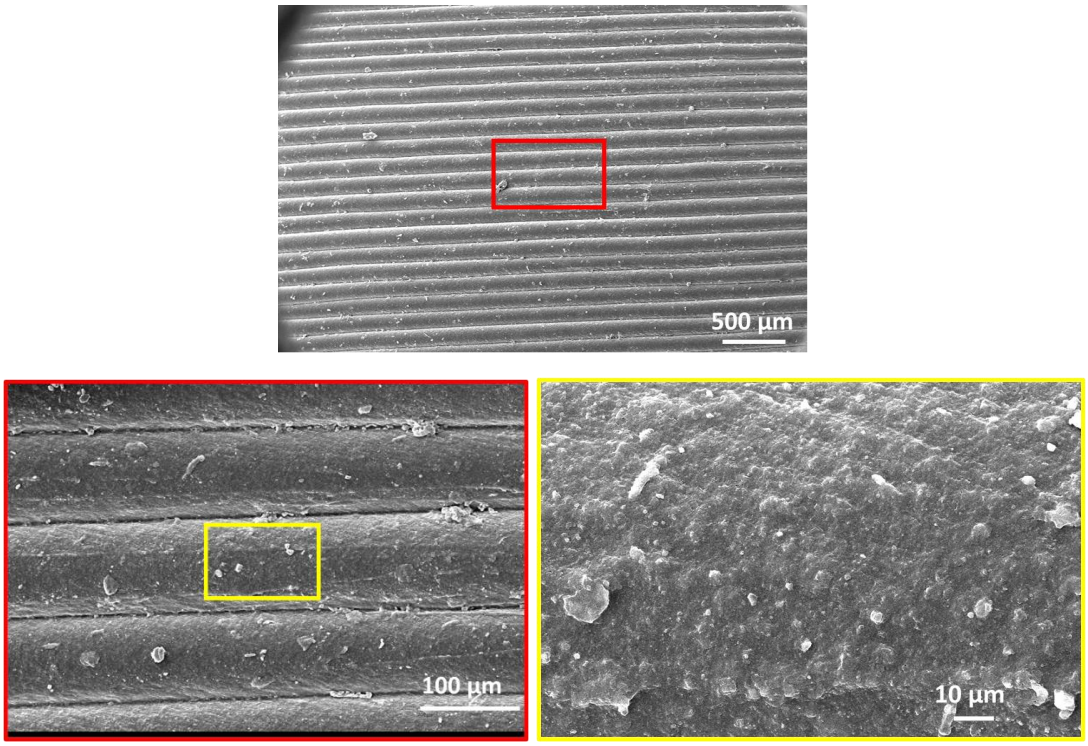

Figure 32: SEM images acquired from the surface of as-printed ABS sample

However, the examination of the surface of a single ABS fiber shown in Figure 33 (as shown in the enlarged view in yellow) suggests that it was free from any evident signs of air bubbles/porosity, which is unlike the case of PLA. It can be fairly concluded that the impact strength of the material (44.41 MPa) as well as limited number of manufacturing defects helped the hair clipper comb to absorb the impact stress without failure.

Chapter 5

Conclusion and Future Work

In this study, two types of customized hair clipper comb were designed using CAD software ONSHAPE, one having a solid body and the other with a hollow. Finite Element analysis was done on both designs using the explicit dynamics module in ANSYS (version 17.2) for drop test using PLA (polylactic Acid) and ABS (acrylonitrile butadiene styrene) as printing materials. Solid model and shell model were dropped in both leg and head orientations using PLA and then ABS material which makes a total of 8 cases. The maximum stresses obtained in numerical analysis were comparable to the UTS of PLA and ABS except in case of head and leg drop of solid design using PLA where the maximum stress (60.3 MPa) exceeds the UTS of PLA (59.2 MPa) due to which the numerical results predict fracture. The results were validated using a drop test conducted from the height of 5 ft. and it was verified that in case of solid design, for both head and leg drop the crack originated exactly from the area where the maximum stress was observed in the numerical simulations. The fractured surface morphology of PLA sample and surface of ABS in as-printed condition were analyzed using scanning electron microscopy. In case of PLA sample, obvious signs of uniformly spread internal porosity and a flat fracture surface characteristic of brittle failure was observed. Facilitated by internal fibre failure, the crack originated from the sharp corner region experiencing highest stress as suggested by the impact test simulation. Clear signs of porosity perpendicular to the direction of extrusion were visible, due to which the surface appearance was non homogenous, and the corresponding porosity indicates that most likely the defects were induced during the manufacturing of PLA filament. While analyzing the ABS fibers there was no porosity observed.

Better and optimized results can be achieved in future studies by using higher values of extrusion width which in our study was not possible because of limitations of 3D printing machine available. Moreover, different raster orientation, i.e. 90° & 0° which from literature suggests have greater impact on mechanical strength, can be used for further

investigations on the impact strength of the hair clipper comb. It would be an interesting study to simulate and assess the suitability of other 3D printable (PETG, Nylon, Carbon fibre) materials for common day applications such as hair clipper comb. More FDM parameters can be used such as layer height, printing speed, build orientations etc. to understand their effect on mechanical behavior of the component upon impact.

References:

[1] R. D. Goodridge, C. J. Tuck, and R. J. M. Hague, “Laser sintering of polyamides and other polymers,” *Prog. Mater. Sci.*, vol. 57, no. 2, pp. 229–267, 2012, doi: 10.1016/j.pmatsci.2011.04.001.

[2] N. T. Aboulkhair, M. Simonelli, L. Parry, I. Ashcroft, C. Tuck, and R. Hague, “3D printing of Aluminium alloys: Additive Manufacturing of Aluminium alloys using selective laser melting,” *Prog. Mater. Sci.*, vol. 106, no. May, p. 100578, 2019, doi: 10.1016/j.pmatsci.2019.100578.

[3] S. L. Sing, J. An, W. Y. Yeong, and F. E. Wiria, “Laser and electron-beam powder-bed additive manufacturing of metallic implants: A review on processes, materials and designs,” *J. Orthop. Res.*, vol. 34, no. 3, pp. 369–385, 2016, doi: 10.1002/jor.23075.

[4] Z. X. Khoo *et al.*, “3D printing of smart materials: A review on recent progresses in 4D printing,” *Virtual Phys. Prototyp.*, vol. 10, no. 3, pp. 103–122, 2015, doi: 10.1080/17452759.2015.1097054.

[5] T. D. Ngo, A. Kashani, G. Imbalzano, K. T. Q. Nguyen, and D. Hui, “Additive manufacturing (3D printing): A review of materials, methods, applications and challenges,” *Compos. Part B Eng.*, vol. 143, no. December 2017, pp. 172–196, 2018, doi: 10.1016/j.compositesb.2018.02.012.

[6] N. I. Jaksic and P. D. Desai, “Characterization of 3D-printed capacitors created by fused filament fabrication using electrically-conductive filament,” *Procedia Manuf.*, vol. 38, no. 2019, pp. 33–41, 2019, doi: 10.1016/j.promfg.2020.01.005.

[7] P. B.A, L. N, A. Buradi, S. N, P. B L, and V. R, “A comprehensive review of emerging additive manufacturing (3D printing technology): Methods, materials, applications, challenges, trends and future potential,” *Mater. Today Proc.*, vol. 52, no. November, pp. 1309–1313, 2022, doi: 10.1016/j.matpr.2021.11.059.

[8] A. Alafaghani, A. Qattawi, B. Alrawi, and A. Guzman, “Experimental Optimization of Fused Deposition Modelling Processing Parameters: A Design-

for-Manufacturing Approach," *Procedia Manuf.*, vol. 10, pp. 791–803, 2017, doi: 10.1016/j.promfg.2017.07.079.

[9] A. Le Duigou, D. Correa, M. Ueda, R. Matsuzaki, and M. Castro, "A review of 3D and 4D printing of natural fibre biocomposites," *Mater. Des.*, vol. 194, p. 108911, 2020, doi: 10.1016/j.matdes.2020.108911.

[10] D. Farbman and C. McCoy, "Materials testing of 3D printed ABS and PLA samples to guide mechanical design," *ASME 2016 11th Int. Manuf. Sci. Eng. Conf. MSEC 2016*, vol. 2, pp. 1–12, 2016, doi: 10.1115/MSEC2016-8668.

[11] A. A. Chevrychkina, G. A. Volkov, and A. D. Estifeev, "An experimental investigation of the strength characteristics of ABS plastic under dynamic loads," *Procedia Struct. Integr.*, vol. 6, pp. 283–285, 2017, doi: 10.1016/j.prostr.2017.11.043.

[12] K. Raney, E. Lani, and D. K. Kalla, "Experimental characterization of the tensile strength of ABS parts manufactured by fused deposition modeling process," *Mater. Today Proc.*, vol. 4, no. 8, pp. 7956–7961, 2017, doi: 10.1016/j.matpr.2017.07.132.

[13] E. Atzeni *et al.*, "Additive manufacturing as a cost-effective way to produce metal parts," *High Value Manuf. Adv. Res. Virtual Rapid Prototyp. - Proc. 6th Int. Conf. Adv. Res. Rapid Prototyping, VR@P 2013*, no. January, pp. 3–8, 2014, doi: 10.1201/b15961-3.

[14] W. Yang and R. Jian, "Advanced Industrial and Engineering Polymer Research Research on intelligent manufacturing of 3D printing / copying of polymer," *Adv. Ind. Eng. Polym. Res.*, vol. 2, no. 2, pp. 88–90, 2019, doi: 10.1016/j.aiepr.2019.03.001.

[15] D. O. Kazmer and A. Colon, "Injection printing: additive molding via shell material extrusion and filling," *Addit. Manuf.*, vol. 36, no. May, 2020, doi: 10.1016/j.addma.2020.101469.

[16] L. T. Sin and B. S. Tueen, "Injection Molding and Three-Dimensional Printing of

Poly(Lactic Acid)," *Polylactic Acid*, pp. 325–345, 2019, doi: 10.1016/b978-0-12-814472-5.00010-8.

[17] S. Kashyap and D. Datta, "Process parameter optimization of plastic injection molding: a review," *Int. J. Plast. Technol.*, vol. 19, no. 1, pp. 1–18, 2015, doi: 10.1007/s12588-015-9115-2.

[18] E. Atzeni, L. Iuliano, P. Minetola, and A. Salmi, "Redesign and cost estimation of rapid manufactured plastic parts," *Rapid Prototyp. J.*, vol. 16, no. 5, pp. 308–317, 2010, doi: 10.1108/13552541011065704.

[19] M. Jiménez, L. Romero, I. A. Domínguez, M. D. M. Espinosa, and M. Domínguez, "Additive Manufacturing Technologies: An Overview about 3D Printing Methods and Future Prospects," *Complexity*, vol. 2019, 2019, doi: 10.1155/2019/9656938.

[20] Sculpteo, "The state of 3D printing 2020," p. 23, 2020.

[21] M. Pérez, D. Carou, E. M. Rubio, and R. Teti, "Current advances in additive manufacturing," *Procedia CIRP*, vol. 88, pp. 439–444, 2020, doi: 10.1016/j.procir.2020.05.076.

[22] M. A. Hossain, A. Zhumabekova, S. C. Paul, and J. R. Kim, "A review of 3D printing in construction and its impact on the labor market," *Sustain.*, vol. 12, no. 20, pp. 1–21, 2020, doi: 10.3390/su12208492.

[23] C. Buchanan and L. Gardner, "Metal 3D printing in construction: A review of methods, research, applications, opportunities and challenges," *Eng. Struct.*, vol. 180, no. November 2018, pp. 332–348, 2019, doi: 10.1016/j.engstruct.2018.11.045.

[24] B. Gadagi and R. Lekurwale, "A review on advances in 3D metal printing," *Mater. Today Proc.*, vol. 45, pp. 277–283, 2020, doi: 10.1016/j.matpr.2020.10.436.

[25] V. Chahal and R. M. Taylor, "A review of geometric sensitivities in laser metal 3D printing," *Virtual Phys. Prototyp.*, vol. 15, no. 2, pp. 227–241, 2020, doi:

10.1080/17452759.2019.1709255.

[26] L. E. Murr, “A Metallographic Review of 3D Printing/Additive Manufacturing of Metal and Alloy Products and Components,” *Metallogr. Microstruct. Anal.*, vol. 7, no. 2, pp. 103–132, 2018, doi: 10.1007/s13632-018-0433-6.

[27] J. Xu, J. Zhu, J. Fan, Q. Zhou, Y. Peng, and S. Guo, “Microstructure and mechanical properties of Ti–6Al–4V alloy fabricated using electron beam freeform fabrication,” *Vacuum*, vol. 167, pp. 364–373, 2019, doi: 10.1016/j.vacuum.2019.06.030.

[28] N. A. Charoo *et al.*, “Selective laser sintering 3D printing–an overview of the technology and pharmaceutical applications,” *Drug Dev. Ind. Pharm.*, vol. 46, no. 6, pp. 869–877, 2020, doi: 10.1080/03639045.2020.1764027.

[29] C. Wei and L. Li, “Recent progress and scientific challenges in multi-material additive manufacturing via laser-based powder bed fusion,” *Virtual Phys. Prototyp.*, vol. 16, no. 3, pp. 347–371, 2021, doi: 10.1080/17452759.2021.1928520.

[30] M. Galati and L. Iuliano, “A literature review of powder-based electron beam melting focusing on numerical simulations,” *Addit. Manuf.*, vol. 19, pp. 1–20, 2018, doi: 10.1016/j.addma.2017.11.001.

[31] P. K. Gokuldoss, S. Kolla, and J. Eckert, “Additive manufacturing processes: Selective laser melting, electron beam melting and binder jetting-selection guidelines,” *Materials (Basel).*, vol. 10, no. 6, 2017, doi: 10.3390/ma10060672.

[32] T. Anderson, “The application of 3D printing for healthcare,” *International Hospitals & Healthcare Review*, 2017. .

[33] B. Berman, “3-D printing: The new industrial revolution,” *Bus. Horiz.*, vol. 55, no. 2, pp. 155–162, 2012, doi: 10.1016/j.bushor.2011.11.003.

[34] F. Baumann and D. Roller, “Additive Manufacturing, Cloud-Based 3D Printing and Associated Services—Overview,” *J. Manuf. Mater. Process.*, vol. 1, no. 2, p. 15, 2017, doi: 10.3390/jmmp1020015.

[35] M. Vaezi, H. Seitz, and S. Yang, “A review on 3D micro-additive manufacturing technologies,” *Int. J. Adv. Manuf. Technol.*, vol. 67, no. 5–8, pp. 1721–1754, 2013, doi: 10.1007/s00170-012-4605-2.

[36] G. Suresh, “Summarization of 3D-Printing Technology in Processing & Development of Medical Implants,” *J. Mech. Contin. Math. Sci.*, vol. 14, no. 1, 2019, doi: 10.26782/jmcms.2019.02.00012.

[37] R. B. Kristiawan, F. Imaduddin, D. Ariawan, Ubaidillah, and Z. Arifin, “A review on the fused deposition modeling (FDM) 3D printing: Filament processing, materials, and printing parameters,” *Open Eng.*, vol. 11, no. 1, pp. 639–649, 2021, doi: 10.1515/eng-2021-0063.

[38] A. K. Sood, R. K. Ohdar, and S. S. Mahapatra, “Parametric appraisal of mechanical property of fused deposition modelling processed parts,” *Mater. Des.*, vol. 31, no. 1, pp. 287–295, 2010, doi: 10.1016/j.matdes.2009.06.016.

[39] J. Kang *et al.*, “Custom design and biomechanical analysis of 3D-printed PEEK rib prostheses,” *Biomech. Model. Mechanobiol.*, vol. 17, no. 4, pp. 1083–1092, 2018, doi: 10.1007/s10237-018-1015-x.

[40] P. Parandoush and D. Lin, “A review on additive manufacturing of polymer-fiber composites,” *Compos. Struct.*, vol. 182, no. August, pp. 36–53, 2017, doi: 10.1016/j.compstruct.2017.08.088.

[41] F. P. W. Melchels, J. Feijen, and D. W. Grijpma, “A review on stereolithography and its applications in biomedical engineering,” *Biomaterials*, vol. 31, no. 24, pp. 6121–6130, 2010, doi: 10.1016/j.biomaterials.2010.04.050.

[42] A. W. Gebisa and H. G. Lemu, “Investigating effects of Fused-deposition modeling (FDM) processing parameters on flexural properties of ULTEM 9085 using designed experiment,” *Materials (Basel).*, vol. 11, no. 4, pp. 1–23, 2018, doi: 10.3390/ma11040500.

[43] X. Wang, M. Jiang, Z. Zhou, J. Gou, and D. Hui, “3D printing of polymer matrix composites: A review and prospective,” *Compos. Part B Eng.*, vol. 110, pp. 442–

458, 2017, doi: 10.1016/j.compositesb.2016.11.034.

[44] J. Z. Manapat, Q. Chen, P. Ye, and R. C. Advincula, “3D Printing of Polymer Nanocomposites via Stereolithography,” *Macromol. Mater. Eng.*, vol. 302, no. 9, pp. 1–13, 2017, doi: 10.1002/mame.201600553.

[45] B. Utela, D. Storti, R. Anderson, and M. Ganter, “A review of process development steps for new material systems in three dimensional printing (3DP),” *J. Manuf. Process.*, vol. 10, no. 2, pp. 96–104, 2008, doi: 10.1016/j.jmapro.2009.03.002.

[46] R. Dou, T. Wang, Y. Guo, and B. Derby, “Ink-jet printing of zirconia: Coffee staining and line stability,” *J. Am. Ceram. Soc.*, vol. 94, no. 11, pp. 3787–3792, 2011, doi: 10.1111/j.1551-2916.2011.04697.x.

[47] S. Haeri, “Optimisation of blade type spreaders for powder bed preparation in Additive Manufacturing using DEM simulations,” *Powder Technol.*, vol. 321, pp. 94–104, 2017, doi: 10.1016/j.powtec.2017.08.011.

[48] S. Jang, S. Park, and C. jun Bae, “Development of ceramic additive manufacturing: process and materials technology,” *Biomed. Eng. Lett.*, vol. 10, no. 4, pp. 493–503, 2020, doi: 10.1007/s13534-020-00175-4.

[49] B. Khoshnevis, “Automated construction by contour crafting - Related robotics and information technologies,” *Autom. Constr.*, vol. 13, no. 1, pp. 5–19, 2004, doi: 10.1016/j.autcon.2003.08.012.

[50] T. S. Jang, H. Do Jung, H. M. Pan, W. T. Han, S. Chen, and J. Song, “3D printing of hydrogel composite systems: Recent advances in technology for tissue engineering,” *Int. J. Bioprinting*, vol. 4, no. 1, pp. 1–28, 2018, doi: 10.18063/IJB.v4i1.126.

[51] I. Gibson, D. Rosen, and B. Stucker, “Additive manufacturing technologies: 3D printing, rapid prototyping, and direct digital manufacturing, second edition,” *Addit. Manuf. Technol. 3D Printing, Rapid Prototyping, Direct Digit. Manuf. Second Ed.*, no. 1991, pp. 1–498, 2015, doi: 10.1007/978-1-4939-2113-3.

[52] H. K. Lee, “Effects of the cladding parameters on the deposition efficiency in pulsed Nd:YAG laser cladding,” *J. Mater. Process. Technol.*, vol. 202, no. 1–3, pp. 321–327, 2008, doi: 10.1016/j.jmatprotec.2007.09.024.

[53] I. Gibson, D. Rosen, and B. Stucker, “Additive manufacturing technologies: 3D printing, rapid prototyping, and direct digital manufacturing, second edition,” *Addit. Manuf. Technol. 3D Printing, Rapid Prototyping, Direct Digit. Manuf. Second Ed.*, no. Dmd, pp. 1–498, 2015, doi: 10.1007/978-1-4939-2113-3.

[54] A. Kazemian, X. Yuan, E. Cochran, and B. Khoshnevis, “Cementitious materials for construction-scale 3D printing: Laboratory testing of fresh printing mixture,” *Constr. Build. Mater.*, vol. 145, pp. 639–647, 2017, doi: 10.1016/j.conbuildmat.2017.04.015.

[55] K. O. Deger and A. H. Deger, “An Application of Mathematical Tessellation Method in Interior Designing,” *Procedia - Soc. Behav. Sci.*, vol. 51, pp. 249–256, 2012, doi: 10.1016/j.sbspro.2012.08.154.

[56] R. Minetto, N. Volpato, J. Stolfi, R. M. M. H. Gregori, and M. V. G. da Silva, “An optimal algorithm for 3D triangle mesh slicing,” *CAD Comput. Aided Des.*, vol. 92, pp. 1–10, 2017, doi: 10.1016/j.cad.2017.07.001.

[57] Wikipedia, “Scanning Electron Microscopy,” 1375. https://en.wikipedia.org/wiki/Scanning_electron_microscope.

[58] A. Bogner, P. H. Jouneau, G. Thollet, D. Basset, and C. Gauthier, “A history of scanning electron microscopy developments: Towards ‘wet-STEM’ imaging,” *Micron*, vol. 38, no. 4, pp. 390–401, 2007, doi: 10.1016/j.micron.2006.06.008.

[59] J. Syed, “Scanning Electron Microscopy in Oral Research,” *J. Pakistan Dent. Assoc.*, vol. 26, no. 4, pp. 189–195, 2018, doi: 10.25301/jpda.264.189.

[60] SEM, “Nano Science Instruments.” https://www.nanoscience.com/techniques/scanning-electron-microscopy/.

[61] D. McMullan, “Scanning electron microscopy 1928–1965,” *Scanning*, vol. 17, no. 3, pp. 175–185, 1995, doi: 10.1002/sca.4950170309.

[62] C. G. Golding, L. L. Lamboo, D. R. Beniac, and T. F. Booth, “The scanning electron microscope in microbiology and diagnosis of infectious disease,” *Sci. Rep.*, vol. 6, no. February, pp. 1–8, 2016, doi: 10.1038/srep26516.

[63] Bitesize Bio, “Scanning Electron Microscopy: 6 SEM Sample Preparation Pointers for Successful Imaging,” 2021. https://bitesizebio.com/34150/sem-sample-prep/.

[64] M. Heidari-Rarani, N. Ezati, P. Sadeghi, and M. R. Badrossamay, “Optimization of FDM process parameters for tensile properties of polylactic acid specimens using Taguchi design of experiment method,” *J. Thermoplast. Compos. Mater.*, 2020, doi: 10.1177/0892705720964560.

[65] A. Savvakis, K and Petousis, M and Vairis, A and Vidakis, N and Bikmeyev, “Imece2014-37553 Deposition Modeling Parts,” *ASME 2014 Int. Mech. Eng. Congr. Expo.*, vol. Volume 14, p. V014T11A022--V014T11A022, 2014, [Online]. Available: http://dx.doi.org/10.1115/IMECE2014-37553.

[66] G. A. Munoz, “Lecture 7: Mesh Quality & Advanced Topics,” *ANSYS Inc.*, p. 37, 2015, [Online]. Available: https://www.academia.edu/16970000/MESH_QUALITY_AND_ADVENCED_TOPICS_ANSYS_WORKBENCH_16_0.

[67] K. Gok, S. Inal, A. Gok, and E. Gulbandilar, “Comparison of effects of different screw materials in the triangle fixation of femoral neck fractures,” *J. Mater. Sci. Mater. Med.*, vol. 28, no. 5, pp. 1–7, 2017, doi: 10.1007/s10856-017-5890-y.

[68] S. Farah, D. G. Anderson, and R. Langer, “Physical and mechanical properties of PLA, and their functions in widespread applications — A comprehensive review,” *Adv. Drug Deliv. Rev.*, vol. 107, pp. 367–392, 2016, doi: 10.1016/j.addr.2016.06.012.

[69] M. How, A. Manufacturing, T. Problem, K. Benefits, and E. Customer, “Ansys G ranta MI for Additive Manufacturing,” pp. 1–3.

[70] F. M. Spinning, “Ingeo ™ Biopolymer 6302D Technical Data Sheet,” pp. 1–4.

[71] Q. Z. Fang, T. J. Wang, and H. M. Li, “Large tensile deformation behavior of PC/ABS alloy,” *Polymer (Guildf).*, vol. 47, no. 14, pp. 5174–5181, 2006, doi: 10.1016/j.polymer.2006.04.069.

[72] N. Naveed, “Investigating the material properties and microstructural changes of fused filament fabricated PLA and tough-PLA parts,” *Polymers (Basel).*, vol. 13, no. 9, 2021, doi: 10.3390/polym13091487.

[73] M. Mazumder, R. Ahmed, A. Wajahat Ali, and S. J. Lee, “SEM and ESEM techniques used for analysis of asphalt binder and mixture: A state of the art review,” *Constr. Build. Mater.*, vol. 186, pp. 313–329, 2018, doi: 10.1016/j.conbuildmat.2018.07.126.